THE ASTROPHYSICAL JOURNAL, 403:183–201, 1993 January 20

REFRACTIVE INTERSTELLAR SCINTILLATION OF PULSAR INTENSITIES AT 74 MHz

Y. GUPTA,[1] B. J. RICKETT, AND W. A. COLES
Department of Electrical and Computer Engineering, University of California at San Diego, La Jolla, CA 92093-0407
Received 1992 February 27; accepted 1992 July 28

ABSTRACT

Daily observations of the flux of nine pulsars have been made with a large phased-array at 74 MHz from 1989 January 24 for 400 days. Modulation indices and time scales have been estimated for the variations. The results are in only partial agreement with the variability expected from refractive interstellar scintillation (RISS), The observed modulation indices are above the expectations from a simple Kolmogorov model of interstellar plasma turbulence, particularly for the nearby pulsars with only moderate levels of scattering. These results are in reasonable agreement with earlier observations, but disagree with recent measurements at 610 MHz by Kaspi & Stinebring (1992). A tentative explanation is proposed in terms of a Kolmogorov spectral model with an inner scale cutoff, in which there is an inverse relation between inner scale and local strength of turbulence. This model requires inner scales in the range 10^7 to 10^9 m. The observed time scales are substantially less than expected from the simple model, even though there are large uncertainties in the predictions of the simple model. No straightforward explanation is found for this discrepancy, which is also observed at 610 MHz. The combination of higher than expected modulation indices and shorter than expected time scales is seen in the structure function of flux, as a steep slope near zero time lag. These range from 1.5 to 150 times steeper than the slopes predicted from the simple model. Taking the pulsar time scales to characterize RISS for point sources, we would expect that the corresponding time scales for RISS of compact extragalactic radio sources would also be substantially reduced.

Subject headings: ISM: general — pulsars: general — turbulence

1. INTRODUCTION

Slow fluctuations of pulsar amplitudes have been reported since the early days of pulsar observations (Cole, Hesse, & Page 1970; Rankin, Payne, & Campbell 1974; Helfand, Fowler, & Kuhlman 1977). However, it was considerably later that Sieber (1982) recognized that they were interstellar propagation effects. Subsequently, Rickett, Coles, & Bourgois (1984) explained these as due to refractive interstellar scintillation (RISS), produced by the same spectrum of electron density fluctuations in the interstellar medium (ISM) that is responsible for the well-known diffractive interstellar scintillation (DISS). They gave a first-order theory predicting the time scales and modulation indices for RISS due to propagation through a medium with a simple Kolmogorov power-law spectrum, and pointed out that RISS could be observed in a variety of other compact radio sources. In this paper we report a new series of observations of pulsars at 74 MHz, which were made with the aim of improving our knowledge of the RISS behavior of point sources. Such observations can refine our knowledge of the interstellar electron irregularities, and also refine our predictions of what RISS variations are to be expected from other compact sources. For example, Rickett (1986) gave an approximate model for variations of extragalactic sources on times of months at meter wavelengths and on times of days at centimeter wavelengths, but he used a rather crude model of the RISS behavior of a point source.

Since the identification of slow fluctuations of pulsars with RISS, there have been only a few new observations. Stinebring & Condon (1990) reported a 43 day sequence of observations of a set of 25 pulsars and confirmed the RISS explanation for the fluctuations. They also noted the stability of the very distant pulsars providing evidence for the intrinsic long-term stability of pulsar amplitudes. Their observations were at frequencies of 310, 416, and 750 MHz, for which the predicted time scales were short enough to be seen in 43 days for the nearby pulsars; however, for these same pulsars the bandwidths and integration times were not long enough to completely average out the DISS variations. As a result they could make quantitative estimates of the RISS time scale and modulation index for only a few pulsars. Rickett & Lyne (1990, hereafter R&L) reported 550 days of observations of the Crab pulsar and summarized the published results for other pulsars as estimates of refractive time scales and modulation indices. Kaspi & Stinebring (1992, hereafter K&S) have recently reported more than a year of observations of 14 pulsars at 610 MHz. They concentrated on pulsars with quite strong scattering and so avoided the "leakage" of diffractive scintillation into the intensity time series. They convincingly confirmed that very distant pulsars exhibit very stable fluxes, consistent with time scales much greater than 1 yr, and they were able to measure the RISS parameters of 11 of their pulsars.

Before the work of K&S the reported modulation indices were substantially greater than predictions for a simple Kolmogorov spectrum model (see Fig. 4 of R&L). However, K&S found the discrepancy to be substantially less. Seven of their pulsars gave good agreement with the Kolmogorov predictions and four pulsars gave poor agreement with the predictions. Various modifications of the pure Kolmogorov spectrum have been proposed to explain the enhanced levels of refractive scintillation. Notable among these are the steep spectrum model (Blandford & Narayan 1985; Goodman & Narayan 1985), which predicts 100% refractive intensity modulations, and the inner scale model (Coles et al. 1987), which predicts increasing levels of refractive scintillations with increasing inner scale.

[1] Now at National Centre for Radio Astrophysics, Tata Institute for Fundamental Research, Poona University Campus, Pune 411007, India.

It is important to discriminate between these alternative spectral models as they imply very different physics for the interstellar medium (see Rickett 1990 for a review). The simple Kolmogorov model is based on turbulence theory and is usually interpreted as a velocity cascade of turbulent energy from large scales (on the order of parsecs) to very small scales ($\lesssim 10^8$ m) in the ISM, though it is also possible to have a reverse vorticity cascade. The few published theoretical studies of turbulence in the interstellar plasma have found it hard to explain a cascade over such a wide range of scales. The inner scale model includes a cutoff at an intermediate scale, at which the turbulent energy is dissipated. The associated power dissipation rate increases inversely with inner scale and could become important to the power balance of the ISM, for the smallest inner scales proposed. The steep spectrum models also have a power law for the spectrum of electron density fluctuations but the wavenumber exponent is larger than that for the Kolmogorov case, which is $-11/3$ for a three-dimensional wavenumber. Spectra with exponents steeper than -4 do not necessarily imply a turbulent cascade. The exact shape of the power spectrum is still open to debate and observations of refractive scintillations can provide discriminating tests. With this in mind, a new program for long-term monitoring of pulsar amplitudes was started at University of California, San Diego. Data were collected from 1989 January to 1990 March, using a large 74 MHz antenna array at Fallbrook (California). In this paper we describe the observations and present the results.

2. OBSERVATIONS AND DATA ANALYSIS

2.1. *The Observations*

The Fallbrook antenna is a 73.8 MHz phased array consisting of 128 linearly polarized elements each consisting of eight full-wave dipoles. The antenna and receiver system were designed to study interplanetary scintillation (IPS), which requires a large antenna, but is not affected by confusion and does not require absolute gain calibration. The array covers 32 λ (north-south) by 16 λ (east-west) and has a total collecting area of 8000 m^2. The resulting antenna pattern has a half-power beam width of 1°.75 (N-S) by 3°.5 (E-W) when pointed normal to the array. The beam is steered by 128 digitally controlled phase shifters. The tracking is controlled by an on-site microcomputer that calculates the required phase gradients and updates the phase shifters every 2 minutes. For this series of observations the receiver was a total power receiver with RF bandwidth of 500 kHz. The receiver system included amplifiers distributed in the array and the effective system temperature was 1000–3000 K, dominated by Galactic noise. After detection, the signal was low-pass filtered using a time constant of 1 ms. While observing the pulsars the signal was further filtered with a high-pass filter having a time constant of 4 s, since the low-frequency components are of no interest. While observing the calibration sources no high-pass filtering was applied; but a fixed dc offset was subtracted from the detected signal to keep the average voltage level within the linear range. The signal was frequency modulated and transmitted to the campus laboratory over a leased telephone line. It was then demodulated, smoothed with an 8 ms time constant, digitally sampled at 50 Hz and saved on magnetic tape. The 8 ms time resolution was shorter than the observed pulse durations for all of the pulsars, since they were substantially broadened by interstellar dispersion across our 500 kHz bandwidth. Since we are only interested in the pulse strength, this broadening does not limit the signal to noise ratio. Only if the net pulse duration is longer than about half the pulse period is the signal to noise degraded.

The requirements for an RISS study include a long enough observing span to include many time scales of the process, sufficient integration in time or bandwidth to average out the DISS for each observation, a high antenna sensitivity and a high gain stability. The Fallbrook antenna, no longer in use for IPS, was well suited to the foregoing requirements, except that it was designed without attention to long-term gain stability. The criteria for selecting the pulsars were closely linked to these requirements. The constraint of using 74 MHz made the RISS time scales long, ranging from a few days for the nearest sources to years for the distant heavily scattered sources. We thus chose the nearest pulsars (0.1 to 1.0 kpc), which also helped us meet the sensitivity requirement. This choice makes our observations complementary to those of K&S who concentrated on the more distant objects. For the sake of comparison, some stronger more distant pulsars were also observed, for which the expected time scale was more than 1 yr; for these objects the flux was expected to remain relatively steady over the time period of our observations. After some preliminary observations nine pulsars were selected for observation once each day. Funding limitations restricted the total time span to 14 months. In each observation the pulsars were tracked for 20–40 minutes depending on the number of pulsars and calibration sources in the same region of local sidereal time (LST). Parameters of interest for the observed pulsars are presented in the first five columns of Table 1: the pulsar name, the average flux at 400 MHz, dispersion measure, sweep time across the 500 kHz observing bandwidth, and integration time. The measured 74 MHz flux is also given, and is discussed in § 3.

Twelve strong continuum radio sources were also observed every day to calibrate the pulse intensities. These were sources having flux densities greater than 50 Jy at 74 MHz. A typical calibration sequence consisted of pointing on and off the source to estimate the change in antenna output power caused by the source. The off-source locations were chosen so that the source fell at the second null of the antenna beam pattern in the N-S direction. By choosing off-source positions to both the north and south, we reduced the effects of confusion. The sensitivity of a meter-wavelength filled-aperture such as Fallbrook is in fact limited by confusion. However, since we are looking for amplitude variations on tens of days, it is only the variability of the confusion that is a problem. The observations were performed at the same sidereal time each day, so the chief

TABLE 1

PULSAR PARAMETERS AND THEIR MEASURED 74 MHz FLUX

	ASSUMED PARAMETERS				MEASURED FLUX	
Name	S_{av}^{400} (mJy)	DM (pc cm^{-3})	τ_{disp} (ms)	T (minutes)	S_{av}^{74} (Jy)	Error
P0329 + 54....	1400	26.78	275	40	1.7	12.2%
P0809 + 74....	50	5.76	59	20	3.2	10.9
P0823 + 26....	70	19.46	200	20	0.57	13.0
P0834 + 06....	65	12.86	132	20	2.4	8.9
P0950 + 08....	900	2.97	30	40	2.6	9.3
P1133 + 16....	340	4.85	50	40	1.4	7.8
P1237 + 25....	160	9.3	95	40	0.25	11.5
P1508 + 55....	125	19.6	201	40	1.6	14.3
P1919 + 21....	240	12.43	127	20	3.0	13.8

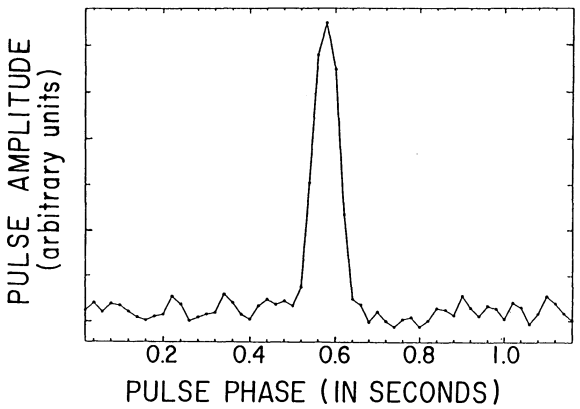

FIG. 1.—Typical daily pulse profile for PSR 1133+16. The pulse amplitude is in arbitrary units. The horizontal scale covers the whole pulse period; the ticks are two sample intervals wide, i.e., 40 ms.

problems were solar confusion and sporadic terrestrial interference. To minimize the effects of ionospheric scintillation, the on-source durations were much longer (typically 8 minutes) than the off-source durations (typically 2 minutes).

2.2. *Pulsar Amplitudes and Calibration*

The raw data for each day's observation of a pulsar were first edited to remove spikes and glitches due to interference and antenna phase updates. The edited data were coherently averaged using the doppler-corrected period of the pulsar to obtain a daily pulse profile. Figure 1 shows a typical pulse profile for PSR 1133+16, which was often the strongest pulsar. The daily pulse profile for day j from pulsar p was fitted with a template of the expected pulse profile, to obtain a least-squares estimate of the pulse strength P_{jp} and its estimation error δP_{jp}. This error only includes processes that fluctuate on a time scale shorter than the pulsar period, since it was obtained from the average profile; see Appendix A for more discussion of the errors. The template was obtained by averaging daily pulse profiles from 20 to 30 days of observations, after they had been properly aligned and scaled.

The estimate of the daily pulse strength was then corrected for time variations of the gain of the antenna and receiver. The measured system gain was found to vary predominantly due to fluctuations of the ambient temperature. This was a consequence of using an unswitched total power receiver, which was not well insulated. After some experimenting, it was found that the gain fluctuations could be adequately modeled as a sinusoidal diurnal variation about a mean value which is allowed to change from day to day to accommodate seasonal variations and degradation of the antenna. Figure 2 shows a typical set of gain data and the fitted model. The model included all the calibration sources observed during each LST day. For each source the daily source strength was estimated as the difference between the average on-source value and the average of the two off-source values. This was normalized by the average value over 12 months of data for that source.

The gain model for a particular 24 hr interval can be written as

$$\hat{G}(t_k) = a \sin(2\pi t_k/T) + b \cos(2\pi t_k/T) + c\,, \qquad (1)$$

where t_k is the LST of observation of the source k and T is 24

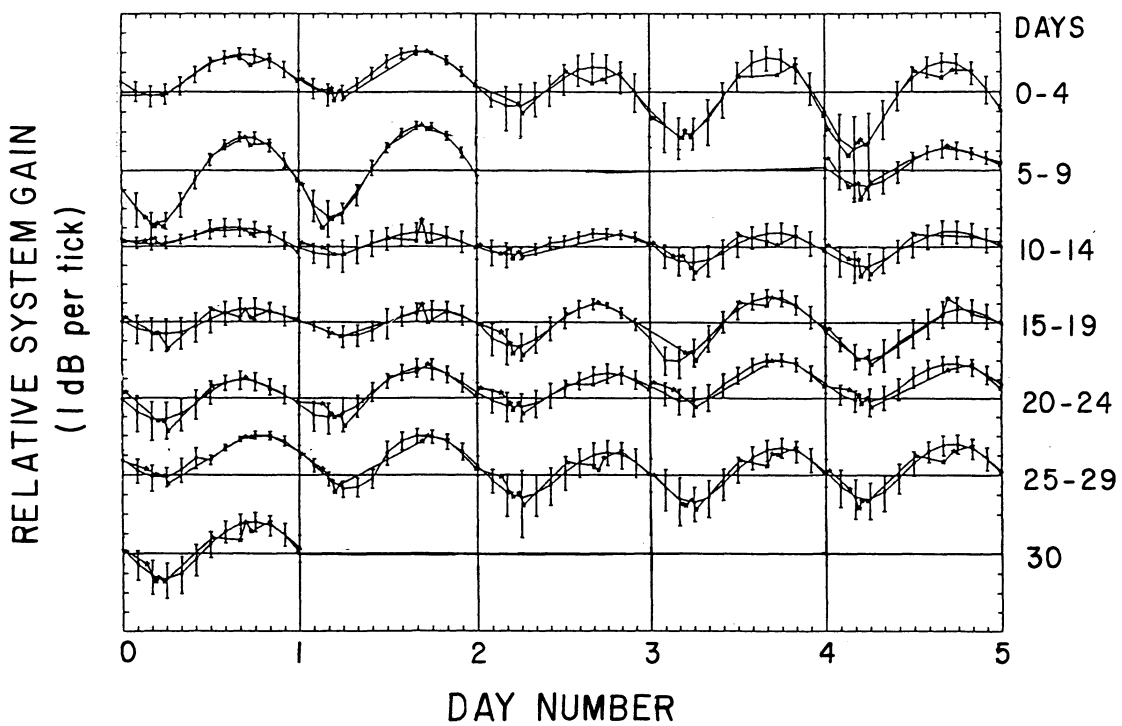

FIG. 2.—Example of the results of system gain estimation using the calibration source observations. The variation of the system gain over a period of 31 days (1989 April 1 to 1989 May 1) is displayed in seven panels, each panel spanning 5 contiguous days. The tick marks on the y-axis show gain changes of 1 dB and those on the x-axis represent time increments of 2 hr. The asterisks (*) mark the data points and the filled circles with the error bars mark the model values, shown at intervals of 2 hr. The blank 2 day section in the second panel corresponds to a time when data were not recorded. The calibration sources were 3C 10, 84, 123, 134, 144, 157, 274, 327, 348, 353, 405 and 461.

hr. The optimum values for the model parameters a, b, and c were obtained by doing a weighted least-squares fit of the gain model to the data points over all the calibration sources available in a 24 hr period. The weights were chosen in the ratio of the square roots of the source fluxes to reduce the vulnerability of the fit to spurious fluctuations of the weaker calibration sources due to solar or terrestrial interference. The choice of a square root weighting was a compromise between emphasizing the stronger sources and maintaining a good distribution of sources over the 24 hr interval. The model was computed for every 24 hr period stepped at 2 hr intervals. For an observation of pulsar p on day j, the system gain $\hat{G}_j(t_p)$ is then given by equation (1) at time t_p of the observation of pulsar p, using the fitted parameters from the 24 hr window centered closest to t_p. The fitting algorithm also calculated the fractional error for each gain estimate, $\delta\hat{G}_j/\hat{G}_j$, derived from the mean squared error between the data and the best-fit model. Since the strong calibration sources were not uniformly spaced in LST, the gain fitting errors varied between pulsars, as illustrated by comparing the error bars on system gain in Figures 3*a* and 3*b*. The final estimate for the corrected daily pulse strength S_{jp} was obtained by dividing each uncorrected pulse strength P_{jp} by the gain $\hat{G}_j(t_p)$. The error δS_{jp} in each value was also computed by combining the errors in the raw pulse strengths and in system gain. The gain correction model was tested by applying the gain model back on the calibration sources themselves. For the stronger calibration sources the residual variations were uncorrelated from day to day, except for a 2%–3% annual variation. For the weaker sources the residuals were larger and overall typical errors in the gain model were estimated at about 8%. This error was typically larger than that due to system noise. Details of the other errors in S are discussed in Appendix A.

The intensity data for pulsars PSR 0329+54 and 1133+16 are shown in Figures 3*a* and 3*b*. The top panel in each figure shows the uncorrected pulsar time series; the second panel shows the estimated system gain; the third panel shows the corrected pulsar intensities; and the fourth panel shows the structure function of the corrected intensities; as discussed below. Notice that short term (5–10 day) fluctuations in the gain curve do not seem to be correlated with fluctuations in the calibrated pulsar intensities. This confirms the success of the gain correction method. We also estimated the off-pulse noise power for each observation and found no significant correlation between it and the calibrated pulsar intensity. The error bars for each time series are $\pm 2\,\sigma$ wide and were estimated as explained above. Note that the error bars for the corrected intensity series only include δS_{jp} (sum of corresponding nvar and gvar values), and so do not include the other short-term noise processes discussed in Appendix A.

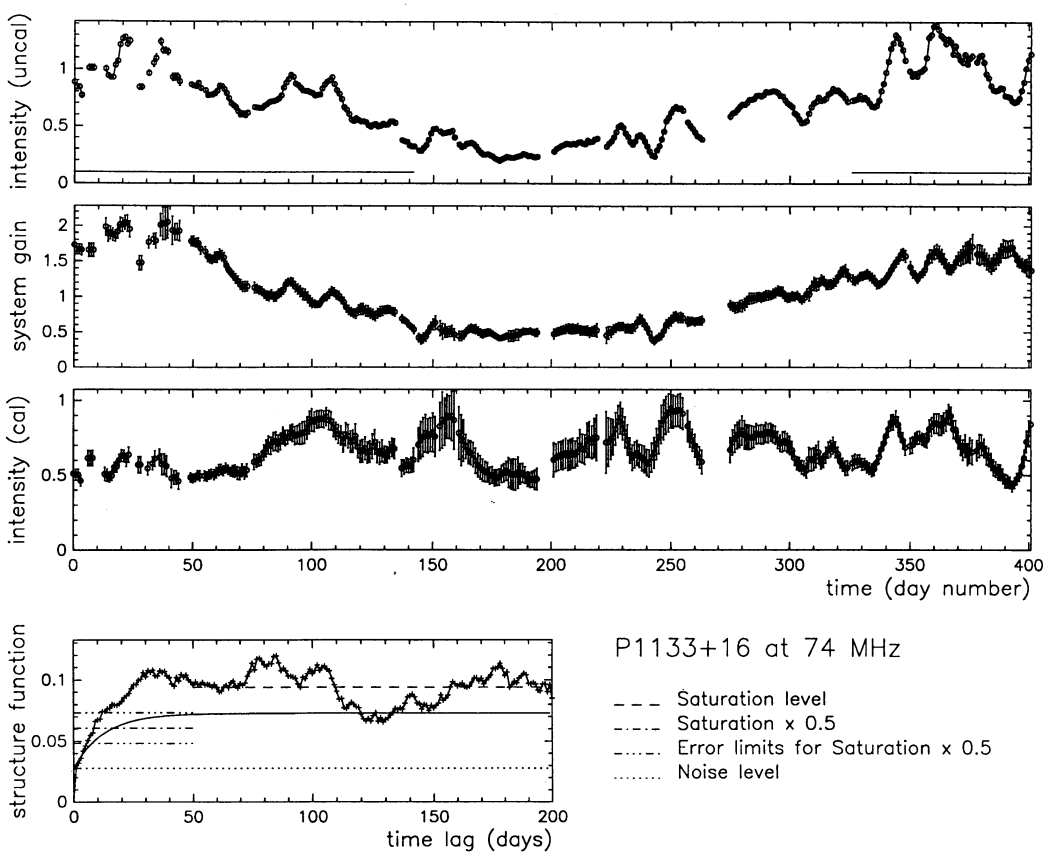

FIG. 3*a*

FIG. 3.—Data for (*a*) PSR 1133+16 and (*b*) PSR 0329+54 showing daily uncalibrated pulse intensity (*top panel*), system gain estimate (*second panel*), gain calibrated pulse intensity (*third panel*) and its structure function (*bottom panel*) from 1989 January 24 to 1990 March 1. The horizontal line in the top panel indicates dates for which the observations were taken at night, between local times 6 am (*at left-hand end*) and 6 pm (*at right-hand end*). The three time series have been smoothed with a 5 day running mean for display purposes, and the error bars are $\pm 2\,\sigma$, for the smoothed time series. The structure functions were computed before smoothing. The smooth solid line is an exponential model for the structure function, with the predicted Kolmogorov variance and time scale.

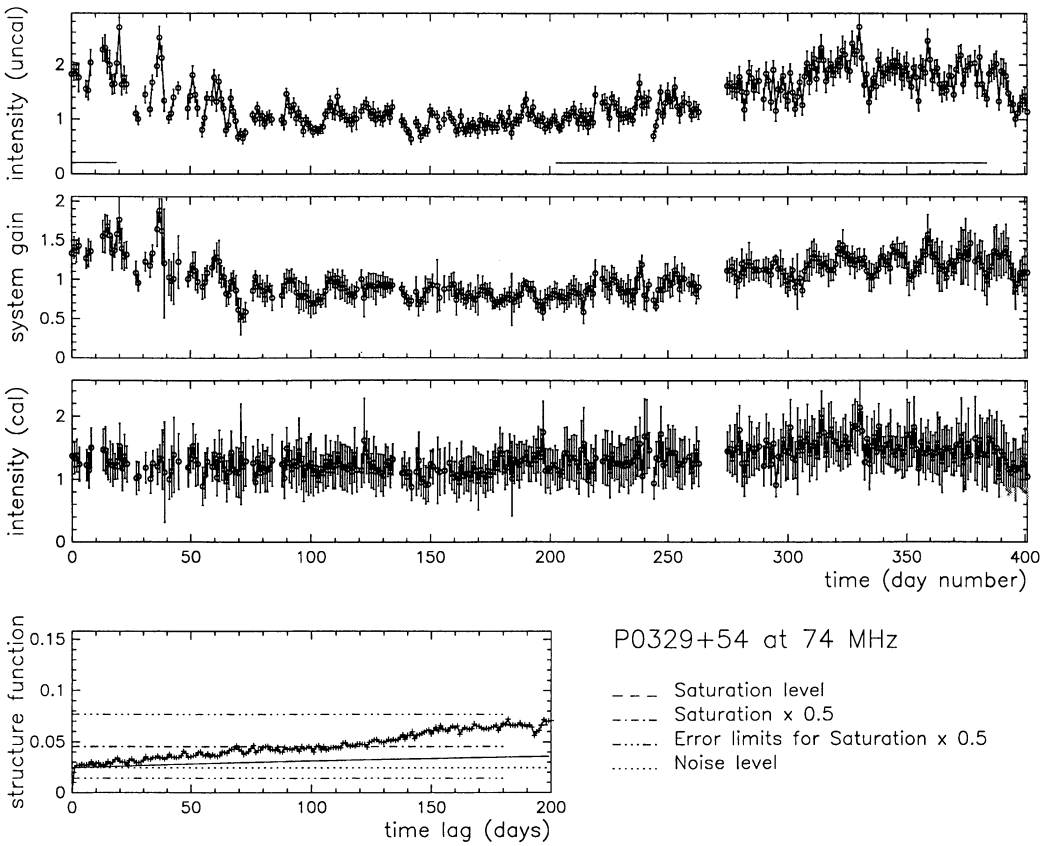

FIG. 3*b*

2.3. *Analysis of the Pulsar Intensity Time Series*

To estimate the time scale and modulation index of refractive scintillations, one can use either the covariance function or the structure function of the data. We found the structure function more useful and use this statistic in the following work. The structure function of pulsar flux $S(t)$ is defined as

$$D_S(\tau) = \langle [S(t) - S(t+\tau)]^2 \rangle = 2[C_S(0) - C_S(\tau)] , \quad (2)$$

where $C_S(\tau)$ is the auto-covariance of S. The ensemble averaged $D_S(\tau)$ rises from zero at zero lag to saturate at twice the total variance at very large lags.

In our computation, D_S for each pulsar includes the variance due to the process of interest (signal) as well as that due to all other processes (noise). The effects of the latter have to be corrected. They comprise all processes that contribute to the day-to-day fluctuation of the corrected intensity time series. These include system noise, varying faraday rotation in the ionosphere, intrinsic pulse-to-pulse fluctuations, diffractive ISS effects, ionospheric and interplanetary scintillations, and errors in the system gain estimate. With the exception of the gain error, these processes are expected to be uncorrelated from one day to the next, thus their effect is confined to a step in the structure function between a lag of zero and one day. Since several of the possible errors are likely to be related to local time, we have included a horizontal bar on the time series plots, that indicate the dates for which the observations were taken at night. This night-time period might have less terrestrial interference, the daytime period might have a greater day to day variability of the Faraday rotation, the dawn and dusk periods might have increased ionospheric scintillation. The system gain is certainly correlated with the ambient temperature which also depends on local time. The corrected flux for the pulsars in Figure 3 do not show any relation with local time. The rest of the flux time series are displayed in Figure 4 and are also unrelated to local time, except in the case of PSR 0809+74, which has higher amplitudes during the night-time observations; in view of the lack of any such effect for the other sources, we presume that this correlation is fortuitous.

As discussed in Appendix A, the total "noise" contribution was estimated as the value of the structure function at unit lag. This value was subtracted from the total structure function to yield the structure function of the signal. This method tends to overcorrect for the noise contribution, since it removes some of the signal too. The effect, however, is slight except for PSR 0950+08, for which the structure function rises abruptly to a value much greater than the estimated noise level, and we conclude that there are real intensity fluctuations that have a time scale of 1–3 days for this pulsar.

There is also a correction to be made to D_S due to the possibility of errors in the system gain estimate that are correlated over several days. As can be seen in Figure 3, the gain function has a noticeable variability on a time scale of 2–5 days. This suggests that there might be gain correction errors correlated over similar times. We estimated the structure function from the residuals for the calibration sources; but this did not lead to a stable function that we could use to correct the D_S estimates. In Table A1 of Appendix A the quantity "gvar" is our estimate of the rms error in the gain correction, which we include in the "noise" that varies from day to day. However, it is likely that part of this variance correlates over a few days.

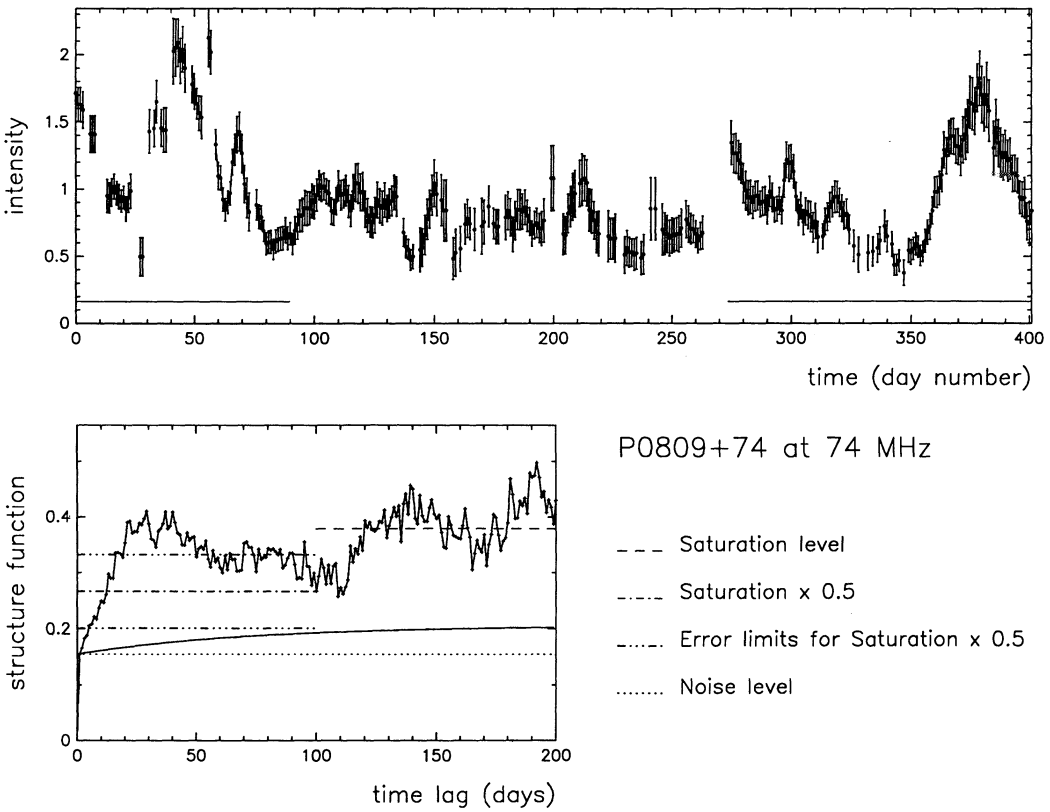

FIG. 4a

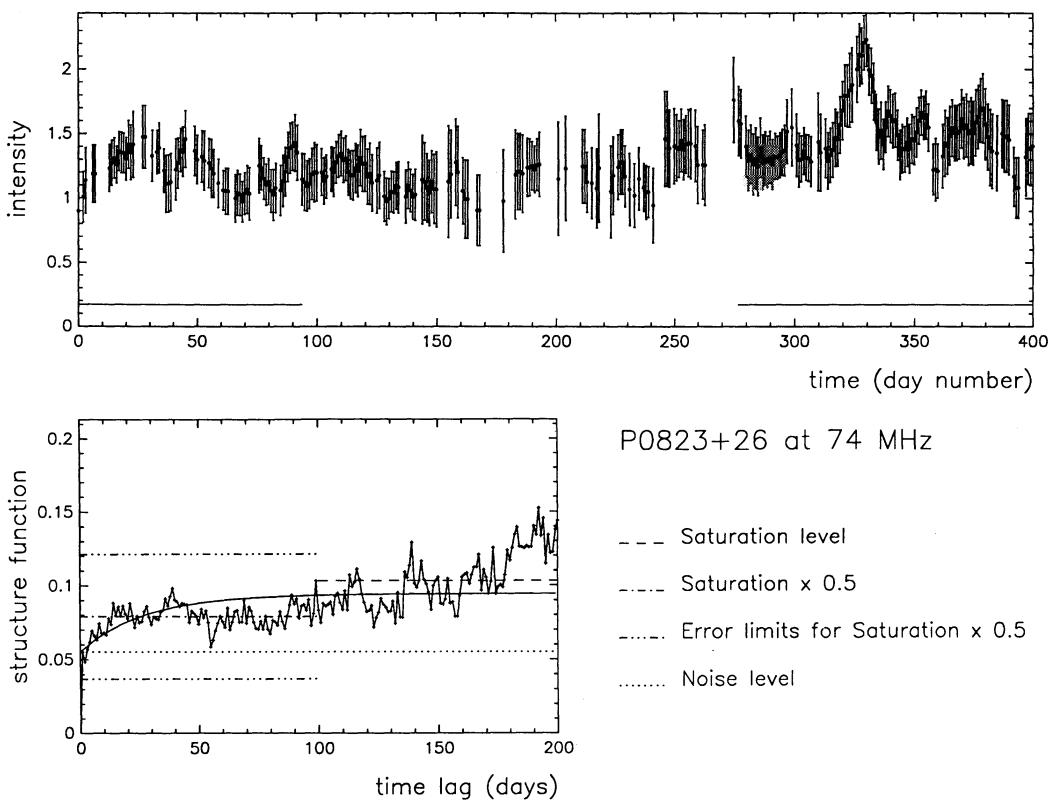

FIG. 4b

FIG. 4.—(*a–g*) Time series of gain calibrated daily pulse intensity vs. day number from 1989 January 24 to 1990 March 1 and the structure function of intensity. (*a*) PSR 0809+74, (*b*) PSR 0823+26, (*c*) PSR 0834+06, (*d*) PSR 0950+08, (*e*) PSR 1237+25, (*f*) PSR 1508+55, (*g*) PSR 1919+21. The horizontal line in the top panel indicates dates for which the observations were taken at night, between local times 6 am (*at left-hand end*) and 6 pm (*at right-hand end*). The time series have been smoothed with a 5 day running mean for all pulsars except PSR 0950+08, for which a 3 day running mean was used. The intensity error bars are $\pm 2\ \sigma$, for the smoothed series. The structure functions were computed before smoothing. The smooth solid line is an exponential model for the structure function, with the predicted Kolmogorov variance and time scale.

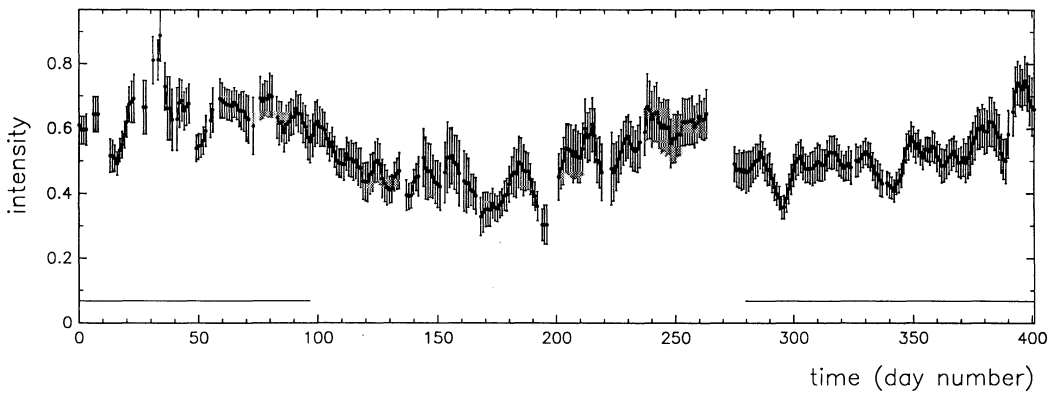

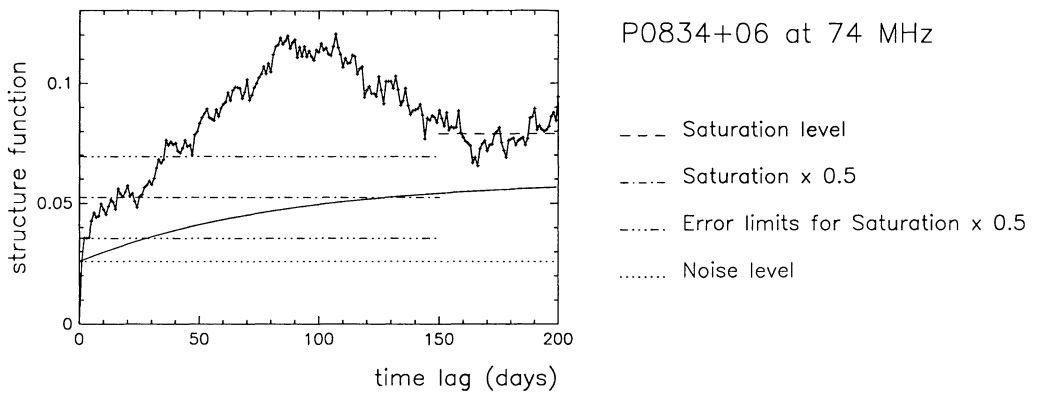

FIG. 4*c*

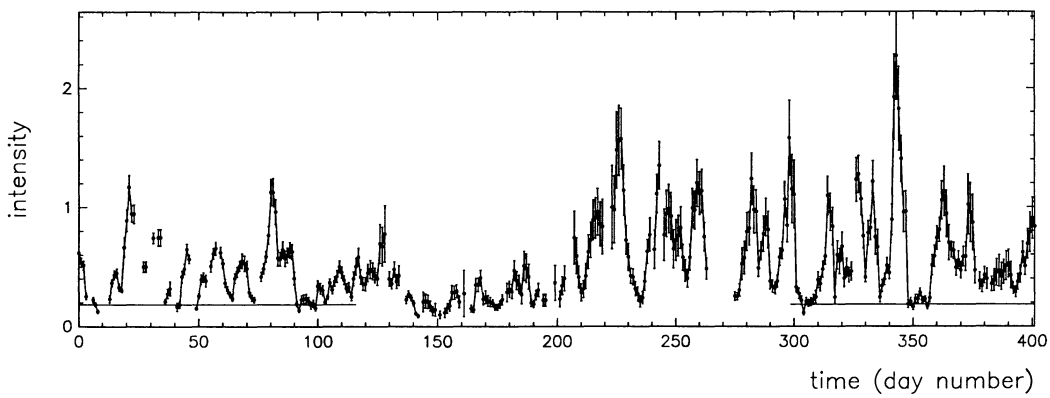

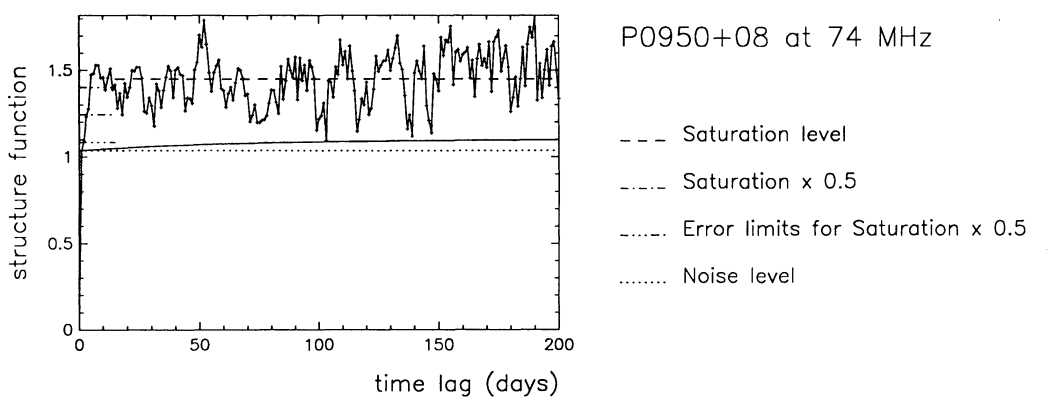

FIG. 4*d*

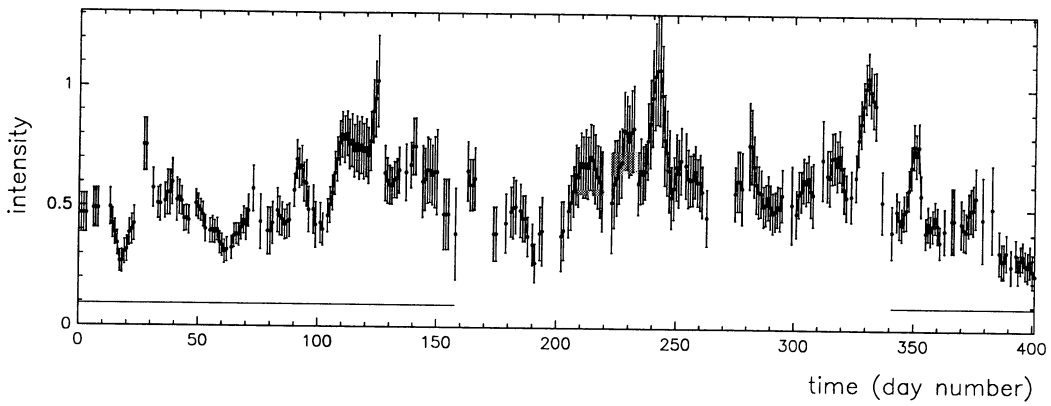

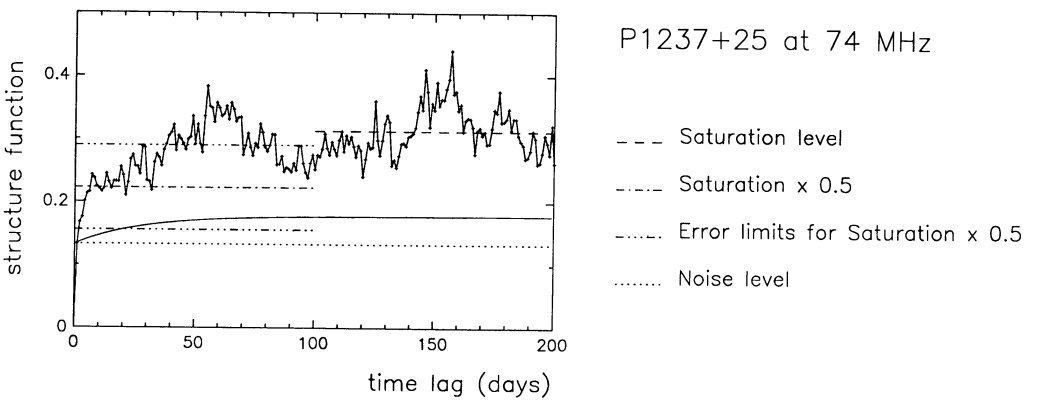

FIG. 4*e*

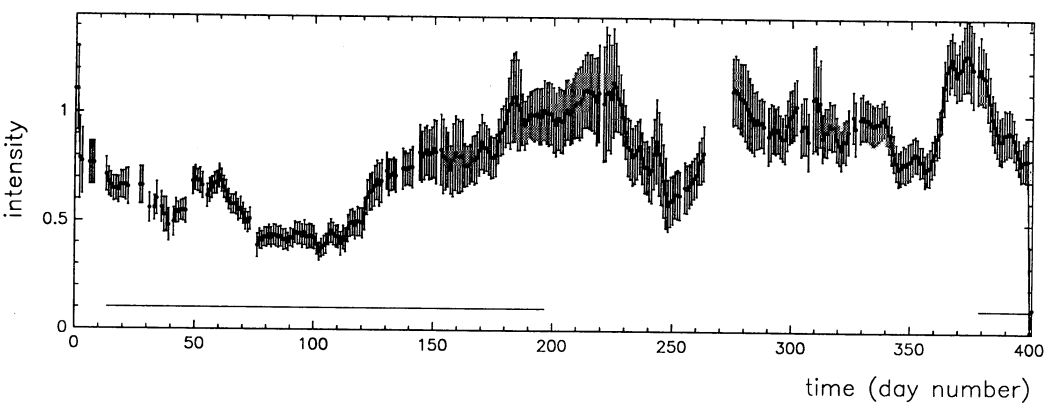

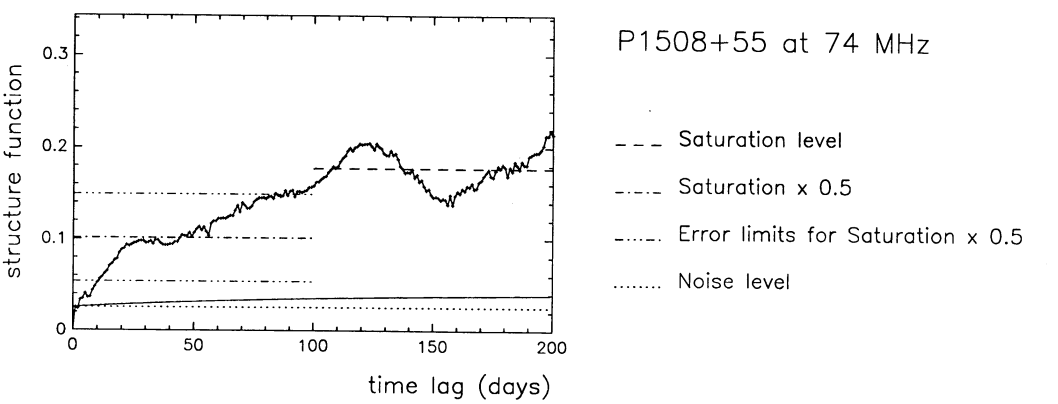

FIG. 4*f*

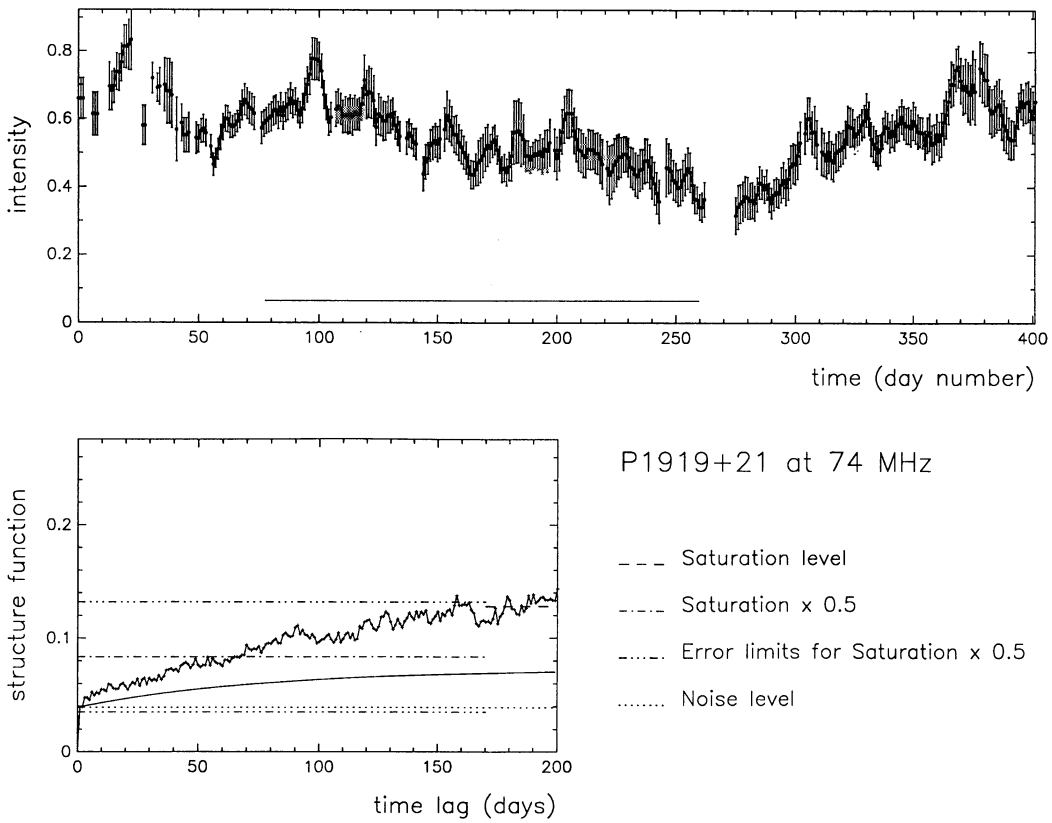

FIG. 4*g*

Since the gain errors are less than 10%, we can linearize their effect such that their main contribution to D_S is a small amplitude additive term proportional to the structure function in the gain errors. For many of the pulsars there is a small amplitude feature in D_S rising over 3–5 days, which we interpret as due to gain errors and not to a real low-amplitude pulsar flux variation. By reference to Table A1 we note that this term should be no greater than about 0.01, but could well lead to noticeable fluctuations with an rms amplitude of $\sqrt{(0.01/2)} = 0.07$ in the pulsar time series.

Our goal is to measure the modulation index and time scale of the variations and to compare them with those predicted by the RISS theory. The modulation index for the intensity is estimated as the square root of half the saturation value of the corrected structure function, provided the original time series is normalized by its mean value. The time scale is estimated as the lag at which the structure function reaches half its saturation value. In practice, we estimate the range of lags over which the structure function is approximately saturated. The average over this range gives an estimate of twice the variance of the fluctuations in S. We now draw a line at half this level and take where it intersects the structure function as an estimate of the time scale. The error range in the level of D_S then maps to an error range for the time scale. This technique and the associated errors were described in more detail by R&L. Figures 4*a*–4*g* show the time series and structure functions for the seven pulsars not displayed in Figure 3. The structure functions are calculated up to a maximum lag of half the data span. For some of the pulsars the structure functions are still increasing at this maximum lag. Only lower bounds for the time scale and modulation index can then be obtained. However, for these pulsars we can still estimate the slope of D_S at zero lag quite accurately, and so we include this parameter in our model comparisons. For other pulsars the structure function starts to cross into saturation but exhibits large oscillations instead of saturating at a final value. This is typically when the data span includes more than one—but not very many—time scales. Here the exact choice of the lags for saturation greatly influences the estimates of time scale and modulation index and the errors associated with them.

The statistical errors in $D_S(\tau)$ are of three types. First there is a white random error, due to estimation error of the "noise" processes. For our 400 days of data the rms of this component is $D_S(1)/\sqrt{400}$. It could be reduced by low pass filtering the time series or by smoothing the structure functions. In Figures 3 and 4 we display the time series smoothed by a running mean, over 3 to 5 days, as noted in the captions. However, the structure functions are computed from the data before smoothing and so preserve the 1 day resolution of the data. The second error contribution in $D_S(\tau)$ is due to estimation errors in the gain correction which were correlated over a few days. As discussed above, we were unsuccessful in correcting for the bias due to gain errors and so cannot reliably model the associated random errors in D_S, but we note that their rms amplitude should be less than gvar (in Table A1) and they should be correlated over lags of few days. The third error contribution to $D_S(\tau)$ comes from the random nature of RISS sampled over a finite observing span $T = 400$ days. For time lags $\tau > \tau_r$ the true structure function should saturate but there will be fluctuations correlated over τ_r, with an rms fractional error of $\simeq\sqrt{\tau_r/T}$. For $\tau < \tau_t$, where the structure function is still an increasing function of τ, the error remains correlated over τ_r,

but the rms fractional error is roughly $\sqrt{\tau/T}$. Formally the errors in this regime depend on the form of $D_S(\tau)$, and the foregoing result applies when $D_S(\tau)$ is asymptotically linear. Some examples of simulations of the estimation errors in a similar structure function are given by Coles et al. (1991) in their figures B1 and B2.

3. RESULTS

As can be seen from Figures 3 and 4, the pulsars exhibit a wide range of time scales and levels of modulation, ranging from the short time scale, large-amplitude fluctuations of PSR 0950+08 to the long time scale, low-level fluctuations of PSR 0329+54. Table 2 summarizes the quantitative results, in comparison with the expected values of time scale τ_r and modulation index m_r. These were derived using the following equations valid for an extended medium model and a Kolmogorov spectrum without an inner scale (Rickett et al. 1984; Coles et al. 1987):

$$\tau_r = \frac{0.5 Z \theta_o}{V} = \frac{0.5}{V}\sqrt{\frac{cZ}{\pi \delta\nu_d}} \quad (3)$$

$$\tau_r = 0.035\ \lambda_m^{2.2} Z_{\rm kpc}^{0.5} \nu_{\rm obs}^{2.2} \delta\nu_{\rm kHz}^{-0.5} V_{\rm kms}^{-1}\ ({\rm days})\ . \quad (3a)$$

$$m_r = 1.21(\delta\nu_d/2\nu)^{0.17} \quad (4)$$

$$m_r = 8.6\ \lambda_m^{-0.57} \nu_{\rm obs}^{-0.73} \delta\nu_{\rm kHz}^{0.17}\ . \quad (4a)$$

In the above equations λ is the wavelength (λ_m in meters), Z is the distance from the pulsar to the observer ($Z_{\rm kpc}$ in kpc), θ_o is the angular radius of the scattering disk, $\delta\nu_d$ is the measured decorrelation bandwidth ($\delta\nu_{\rm kHz}$ in kHz) and V ($V_{\rm kms}$ in km s^{-1}) is the total relative velocity between the scintillation pattern and the observer. For pulsars this velocity is usually dominated by the large proper motion of the source. Observations of $\delta\nu_d$ are typically made at frequencies higher than that used for m_r. Thus in equation (3a) we include the frequency-scaling laws to give the refractive time scale at wavelength λ_m in terms of $\delta\nu_{\rm kHz}$ observed at frequency $\nu_{\rm obs}$ (in MHz). Similarly, equation (4) for the modulation index has been re-expressed as the refractive modulation index at λ_m in terms of $\delta\nu_{\rm kHz}$ observed at frequency $\nu_{\rm obs}$ (in MHz) in equation (4a). In Table 2 the values for $\delta\nu_{\rm kHz}$ correspond to 1 GHz and are taken from Cordes (1986). Where possible values for V are taken from proper motion studies (Lyne, Anderson, & Salter 1982) otherwise from Cordes (1986). Z is taken from a table of pulsar parameters (Manchester & Taylor 1981).

Theoretical expressions similar to equations (3) and (4) are used in the recent study by K&S. Their expression for m_r agrees within 2%, but their expression for τ_r includes a factor K, which when evaluated for equation (3) is equal to 3.1. As a consequence their predicted time scales are 3.1 times shorter than ours. This matter is raised again in § 4. Our predicted time scales range from 18 days to 324 days and the modulation indices range from 0.09 (9% rms fluctuation) to 0.18 (18% rms fluctuation). It should be noted that the uncertainty in the values of V can be a major cause for errors in the theoretical estimates of the time scales. This is particularly important for pulsars where this proper motion velocity is small and comparable to other relevant velocities (e.g., the orbital motion of the earth and the peculiar motion of the Sun).

To give a visual comparison of observations and theory, the structure function plots include a smooth solid line representing an approximate (exponential) model for the structure function, parameterized by the predicted m_r and τ_r: $2\,m_r^2\,\{1 - \exp[-t(\ln 2)/\tau_r]\}$. The data generally lie above this line and rise more quickly. The estimated values for m_r and τ_r are listed in Table 2. For three of the pulsars (PSR 0809+74, 0950+08, and 1133+16) the measurements are reasonably well determined; for four pulsars (PSR 0823+26, 0834+06, 1237+25, and 1508+55) the time scale is very poorly determined and for two pulsars (PSR 0329+54 and 1919+21) only limits were obtained. In order to extract the maximum information in these latter cases, we also list the slope of the structure function extrapolated to zero lag. This quantity is particularly useful when the structure function does not saturate over the available lags. An approximately linear segment of the D_S plots was selected by eye. A line was drawn through the structure function over this range of lags, denoted as 1 day to 2 $t_{\rm slope}$ days. The slope of this line is entered in Table 2. The predicted errors in the slopes come from a fractional error of $(t_{\rm slope}/400)^{0.5}$. It gives the statistical error under the assumption that the structure function is exponential in form; we guess that the noise and systematic errors are of a similar magnitude. The predicted slope is tabulated as $2m_r^2/\tau_r$, and is discussed further in the final section. From Table 2 we see that the observed slopes are all greater than expected—by factors from 1.5 to 150. We now discuss the results for each pulsar in detail.

TABLE 2

PREDICTED AND MEASURED RISS PARAMETERS AT 74 MHz

ASSUMED PARAMETERS				PREDICTED PARAMETERS[a]			MEASURED PARAMETERS		
Name	Z (kpc)	$\delta\nu_{d,1\,\rm GHz}$ (MHz)	V (km s^{-1})	τ_r (days)	m_r	$dD_s/d\tau$ (day^{-1})	τ_r (days)	m_r	$dD_s/d\tau$ (day^{-1})
P0329+54.....	2.30	3.9	229	324	0.098	5.9×10^{-5}	>100	>0.15 ± 0.06	$(2.3 \pm 1) \times 10^{-4}$
P0809+74.....	0.17	85.	41	105[b]	0.16	4.9×10^{-4}	10.0 ± 6	0.34 ± 0.06	$(1.1 \pm 0.2) \times 10^{-2}$
P0823+26.....	0.71	33.	365	39	0.14	1.0×10^{-3}	[12 ± 6]	[>0.16 ± 0.05]	$(1.7 \pm 0.2) \times 10^{-3}$
P0834+06.....	0.43	26.	104	120	0.13	2.8×10^{-4}	19 ± 16	0.16 ± 0.03	$(9.2 \pm 3) \times 10^{-4}$
P0950+08.....	0.09	162.	23	98	0.18	6.6×10^{-4}	3.2 ± 1.4	0.45 ± 0.05	$(9.7 \pm 0.9) \times 10^{-2}$
P1133+16.....	0.15	60.	264	18	0.15	2.5×10^{-3}	8.7 ± 3.2	0.18 ± 0.02	$(4.1 \pm 0.5) \times 10^{-3}$
P1237+25.....	0.33	62.	178	40	0.15	1.1×10^{-3}	19 ± 18[c]	0.30 ± 0.06	$(1.9 \pm 0.2) \times 10^{-2}$
P1508+55.....	0.73	2.3	346	156[d]	0.090	1.0×10^{-4}	47 ± 37	0.28 ± 0.09	$(3.3 \pm 0.5) \times 10^{-3}$
P1919+21.....	0.33	24.	100	113	0.13	3.0×10^{-4}	>100	>0.21 ± 0.08	$(6.2 \pm 2) \times 10^{-4}$

[a] There are substantial uncertainties in the predicted parameters, as discussed in the text.
[b] An estimate of 47 days comes from an alternative choice of the $\delta\nu_d$ reported by Rickett 1970.
[c] Two scales may be present—≈5 days and ≈30 days.
[d] An estimate of 55 days comes from an alternative choice of the $\delta\nu_d$ reported by Armstrong & Rickett 1981.

3.1. *PSR 0329+54*

The structure function in Figure 3*a* shows no signs of saturation up to the maximum lag of 200 days. The observed slope of the structure function (t_{slope} = 100 days) is 4 times the predicted slope in Table 2, as can also be seen from comparing the observed and predicted structure functions. Using the last 20 lags to bound the maximum value of the structure function, the lower bounds on the time scale and modulation index are 100 days and 0.15 ± 0.06. A much larger span of data is needed to estimate these quantities accurately. The lower bound on the time scale is consistent with the expected time scale of 324 days. The lower bound value for m_r is just greater than 0.1, the value predicted for a simple Kolmogorov spectrum (Table 2).

3.2. *PSR 0809+74*

The time series for this pulsar in Figure 4*a* shows two large fluctuations on time scales of about 20 days, in addition there are many lower amplitude and more rapid variations that are nevertheless above the noise level. The structure function shows clear saturation beyond about 20 days. The estimated time scale is 10 ± 6 days and modulation index is 0.34 ± 0.06. The errors are due to the uncertainty in the estimate of the saturation value caused by the substantial fluctuations of the structure function in the saturation regime. The estimated time scale is very much less than the predicted value of 105 days (Table 2). However, if instead of the Cordes (1986) value for δv_d we use an earlier bandwidth measurement (Rickett 1970) converted as in Cordes, Weisberg, & Boriakoff (1985) to δv_d, the predicted time scale is reduced to 47 days. The estimated m_r value is significantly larger than 0.16, the value predicted for a simple Kolmogorov spectrum. Note that the measured time scale and modulation index are consistent with the values ($\tau_r \approx 20 \pm 6$ days and $m_r \approx 0.45 \pm 0.18$), derived by R&L from the early observations at 81.5 MHz by Cole et al. (1970). The observed slope (t_{slope} = 10 days) is about 20 times steeper than that predicted, reflecting both the large m_r and small τ_r.

3.3. *PSR 0823+26*

The time series for this pulsar in Figure 4*b* show some 10 day fluctuations that are just above the large error bars. The signal-to-noise ratio for PSR 0823+26 is less than for most other pulsars and is responsible for the relatively noisy appearance of its structure function. There are variations on about a 10 day time scale during which the structure function rises to a intermediate level which it maintains till a lag of about 70 days. At greater lags the structure function begins to increase again, indicating that there might possibly be another scale of fluctuations greater than 70 days, which we have not resolved. Concentrating on the short term variation, we estimate its scale as 12 ± 6 days and its modulation index as 0.16 ± 0.05. Though uncertain, the time scale is less than the expected value of 39 days (Table 2), but the modulation index is consistent with the value (0.14) predicted for a simple Kolmogorov spectrum. In view of the possibility of a longer time scale and the poor signal-to-noise ratio for this pulsar, we do not regard the estimated parameters as useful; this is indicated by brackets in Table 2. The observed slope (t_{slope} = 8 days) is somewhat steeper than predicted. However, given the large error bars in the time series, the difference is probably not significant.

3.4. *PSR 0834+06*

The time series for this pulsar in Figure 4*c* show variations on less than 5–10 days superposed on variations over 100 days. The structure function has a large oscillation with a maximum value at about 90 days. The saturation variance is accordingly very unreliable, as are the estimated time scale (19 ± 16 days) and modulation index (0.16 ± 0.03). The time scale is consistent with the value 25 ± 16 days, derived from observations of Cole et al. (1970); however, the modulation index is notably less than their value (0.39 ± 0.11). These estimates for τ_r are much less than the expected value of 120 days (Table 2), while that for m_r is slightly larger than 0.13, the value predicted for a simple Kolmogorov spectrum. For the slope estimate we used t_{slope} = 45 days, on the assumption that the feature rising from 1 to 4 days is due to residual errors in the gain correction. The slope is 3 times that expected, but has a large error.

3.5. *PSR 0950+08*

Of all the pulsars observed, PSR 0950+08 shows the strongest fluctuations (Fig. 4*d*), with peaks as much as twice the mean amplitude, occurring over time scales of 2–5 days. The signal-to-noise ratio for this pulsar is very good and the error bars on these estimates are very small. When compared with the gain fluctuations, there appears to be no correlation between the pulsar fluctuations and the system gain, though they both vary on similar time scales. The structure function has a very large step at unit lag—very much bigger than that expected as listed in Table A1. It then rises over 5 days to a fairly steady albeit "noisy" saturation level. Using the standard method of subtracting the unit lag value of D_S leads to $\tau_r = 3.2 \pm 1.4$ days and $m_r = 0.45 \pm 0.05$. Because of the short time scale the unit lag subtraction method will significantly underestimate the scintillation index and overestimate the scale. As an alternative estimate we subtract twice the total "noise" variance expected from Table A1 and obtain τ_r = 2.5 days and m_r = 0.8, corresponding to an even larger amplitude and a shorter time scale. Our observations are approximately consistent with those of Cole et al. (1970), though their data were smoothed over 7 days and so suppressed the day-to-day fluctuations. The observed m_r is greater than the value 0.18 expected for the simple Kolmogorov spectrum.

More notable still is that our nominal time scale of 3.2 days for this pulsar is totally inconsistent with expected RISS value, which is 98 days (Table 2). This pulsar is special in that it is very close to us (only 90 pc) and has a very small proper motion velocity (only 15 km s^{-1}). In fact, the velocity is so small that the assumption that it dominates the relative velocity between the observer and the scintillation pattern is no longer valid. The annual motion of the Earth around the Sun makes significant changes to the total relative velocity. Using the proper motion measurements of Lyne et al. (1982), assumed to be relative to the Sun, and adding the Earth's vector velocity gives a net transverse velocity that has an average of 23 km s^{-1} (as entered in Table 2). The velocity varies between lows of about 14 km s^{-1} on days of year 140 and 320 and highs of about 33 km s^{-1} on days of year 45 and 215. However, the greatest transverse velocity only shortens the expected time scale by a factor of 1.5, still leaving it a factor 20 longer than the observed time scale. The measured slope of the structure function (t_{slope} = 3 days) is about 0.1 per day which is very much greater than the prediction of 0.0007 per day.

There are in fact two puzzles. The very short fluctuation time and the very large unit lag step (or 1 day variance). The 1 day variance is most likely due to the pulsar's linear polarization and an ionospheric Faraday rotation angle varying from one day to the next. The estimate in Table A1 of the "noise"

variance for this object is dominated by changing Faraday rotation; this predicts a 1 day step of 1.0 in D_S, in agreement with the observed step in Figure 4*d*. The estimated total angle of Faraday rotation is 20 rad (using a rotation measure of 1.3 rad m^{-2}). The ionospheric contribution is about 10 rad and even a 5% fluctuation from day to day would change the angle in equation (A4) by 1 rad and so modulate the apparent flux. According to the results of Schwarz & Morris (1971), such a change would occur rapidly (on time scale of about 10 minutes, when scaled to 74 MHz). Thus the apparent flux should vary independently on successive days. Additional slower fluctuations of rotation angle would not correspond to visible slower variations of apparent flux, since essentially 100% decorrelation over 24 hr is caused by the hourly variations (see Appendix A). Further evidence is given in Figure 4*d* in which we see no sign of increased day-to-day flux variations for data recorded during daylight hours, for which the ionosphere should be more variable. Thus we believe that the substantial fluctuations over 3 days are not due to the ionosphere. However, in view of the strong ionospheric influence on this pulsar, new low-frequency polarimetry on PSR 0950+08 would be of considerable interest.

There remains the question of what causes the substantial (45%) fluctuations over 3 days. These could be intrinsic to the pulsar, but the observed stability of the distant pulsars, such as our data on PSR 0329+54 and those of Stinebring & Condon (1990) on PSR 1818−04, 1933+16 and 2111+46 argues against intrinsic rapid large amplitude variations. There is also the possibility that the RISS model is seriously at fault, particularly in regard to the time scale. The discrepancy by a factor of 20 is by far the greatest in our limited data set, but many of our observations show time scales shorter than expected by factors as great as 5. This issue will be further discussed in our concluding section.

3.6. *PSR 1133+16*

The time series for this pulsar in Figure 3*b* shows several 10 day fluctuations. The measured structure function yields a τ_r of 9 ± 3 days and a m_r of 0.18 ± 0.02. These are the most reliable estimates from our nine pulsars. Though the saturation regime of the structure function seems to be well defined, there are sizable oscillations in the structure function in this region; however, their amplitudes are approximately consistent with those expected from the (400/9) independent variations in our 400 days of data. The estimated τ_r is a factor 2 less than the expected value of 18 days from Table 2. The observations of Cole et al. (1970) yielded a time scale less than about 7 days and $m_r = 0.3$. The observed m_r is only slightly larger than the value of 0.15 predicted for a simple Kolmogorov spectrum. For the slope estimate we used $t_{\rm slope} = 5$ days, which gives a slope only 60% greater than predicted.

3.7. *PSR 1237+25*

Like PSR 0823+26, this pulsar has a poor signal-to-noise ratio but the time series for this pulsar in Figure 4*e* shows 10–30 day fluctuations that are clearly greater than the error bars. In the structure function there is a rapid rise over about 8 days and a slower rise over 50 days and oscillations at large lags. This suggests two time scales but we do not regard the evidence as strong. For a single process we estimate τ_r as 19 ± 18 days and m_r as 0.30 ± 0.06. The time scale is compatible with that predicted from the RISS model (40 days from Table 2) and m_r is larger than 0.15, the value predicted for a simple Kolmogorov spectrum. For the slope estimate we used $t_{\rm slope} = 4$ days, which is the shorter of the two time scales evident in Figure 4*e*, and leads to a slope 20 times the prediction; note that this could be due to residual errors in the gain correction that are correlated over a few days.

3.8. *PSR 1508+55*

The data for this pulsar shows a few slow fluctuations in the time series of Figure 4*f*. Even without any smoothing the data show very small fluctuations over 1–3 days, and the structure function is remarkably smooth on such short scales. It rises to a maximum at a lag of 120 days and starts to oscillate perhaps indicating an approach to saturation. The nominal estimates are $\tau_r = 47 \pm 37$ days and $m_r = 0.28 \pm 0.09$. The former is shorter than the expected τ_r of 156 days (Table 2), and the latter is again larger than 0.10, the value predicted for a simple Kolmogorov spectrum. As in the case of PSR 0809+74, there are conflicting measurements for δv_d. Armstrong & Rickett (1981) reported a value about 8 times larger than Cordes (1986), reducing the predicted time scale to about 55 days. For the slope estimate we used $t_{\rm slope} = 10$ days, giving a slope about 30 times the prediction.

3.9. *PSR 1919+21*

The time series for this pulsar in Figure 4*g* show a long-term fluctuation over 200 days and some short-term variations over about 5 days. The structure function shows a small amplitude (0.01) rise between 1–5 days, that corresponds to the short-term variations in the time series. We assume that these are residual errors in the system gain correction, since they have a similar time scale, but we note that they might alternatively be intrinsic or a rapid component of RISS. We assume that the long-term variations are RISS, but we note that they are somewhat correlated with the annual term in the system gain function and so may be corrupted by improper gain correction. The long-term component appears as the slow rise in the structure function, which does not saturate before the maximum lag value. The slope is reasonably well estimated (over $t_{\rm slope} = 40$ days), and is about twice the predicted slope. Since saturation is not reliably detected, the other parameters can only be bounded. The resulting bounds are $\tau_r > 100$ days and $m_r > 0.21 \pm 0.08$. The first is consistent with the expected time scale of 113 days, while the second is larger than the value (0.13) predicted for a simple Kolmogorov spectrum.

3.10. *Absolute Flux Estimates for the Pulsars*

The long-term observations can also be used to estimate the average flux at 74 MHz for the pulsars. The calibration needed was established from measurements of the continuum sources (of known flux) used for gain calibration. The flux values for each source were corrected for all factors such as antenna pattern and known changes in receiver gain. These were then averaged over one year to reduce the error due to uncertainty in the annual gain fluctuation of the antenna. Some errors remain due to confusion associated with individual calibration sources, particularly for the weaker sources. To account for this we weighted each calibration source by its flux in the least-squares error fit used to determine the absolute flux calibration. Since the pulse strength estimates were already normalized to the area under each pulse template, they were multiplied by the area and divided by the pulsar period. The results for time-averaged pulsar fluxes at 74 MHz are shown in

Table 1. The errors come partly from the relative variability of each pulsar and partly from the uncertainty in the absolute flux calibration.

4. DISCUSSION AND CONCLUSIONS

Daily observations of pulsar flux variations at 74 MHz have been characterized by their structure functions. They have been used, as discussed above, to estimate the modulation index m_r and the time scale τ_r for RISS, which is assumed to be the major component of the variations. In some cases, where the data span was not long enough, we could only estimate lower bounds to these parameters. However we also estimate the slope $[dD_S/d\tau]_{\tau=0}$, which can be estimated even from data spans shorter than τ_r. In some cases there appear to be two time scales in the data. We assume that variations of a few percent over 2–5 days are probably residual errors from the system gain corrections; thus RISS variations over such short times may be corrupted. For variations on time scale of 1 yr there is also a small error possible in the gain correction, which we ignore. For four of the five pulsars also observed by Cole et al. (1970) at 81.5 MHz, our results agree to within the errors (with the parameters estimated by R&L). When compared with the simple Kolmogorov model for RISS, our observed m_r is almost always too great and our observed τ_r is always too short, and the observed slope is always too high. This is consistent with conclusions from several other studies. However, it is not immediately consistent with the results of K&S, who found modulation indices only slightly above the simple Kolmogorov values and time scale both shorter and longer than expected.

4.1. *Refractive Scintillation Index*

The RISS model we are using for comparison is perhaps the simplest one could devise, a uniform distribution of turbulence and a pure Kolmogorov spectrum. In this case the dependence of m_r on distance and level of turbulence reduces to a dependence on the diffractive scintillation quantity $\delta\nu_d/\nu$. This is more useful than distance, because it removes the effect of the large variations of scattering strength between neighboring lines of sight (Cordes et al. 1985). Thus we follow the idea of R&L and plot in Figure 5 our observations of m_r versus the $\delta\nu_d/\nu$ measured for each pulsar and scaled to 74 MHz. To this we have added for comparison the recent results of K&S, and all of the published observations of m_r, as summarized by R&L. The solid line gives the Kolmogorov theory from equation (4). Compare first our results and those of K&S with this line. With one exception the K&S results lie above the Kolmogorov line, but they are all within about two standard deviations of it. In contrast four out of nine of our values and lower limits are significantly above the line. The most obvious difference is that the four high points come from nearby and high-latitude pulsars (PSR 0950+08, 0809+74, 1237+25, and 1508+55), with distances 0.09–0.73 kpc. The earlier observations also show m_r greater than the Kolmogorov prediction, which led Coles et al. (1987) to suggest that adding an inner scale cutoff to the Kolmogorov spectra could produce the enhancement of m_r. As mentioned by R&L, the theoretical m_r values for an inner scale model depend both on $\delta\nu_d/\nu$ and on the fresnel scale. However, they noted that m_r can be approximately plotted against $\delta\nu_d/\nu$, by making use of the distance and wavelength scaling laws. Unfortunately the lines plotted by R&L included an error in the scaling. In Appendix B we explain the corrected theory in detail and equation (B7) gives an explicit expression for m_r. These are plotted as dashed lines

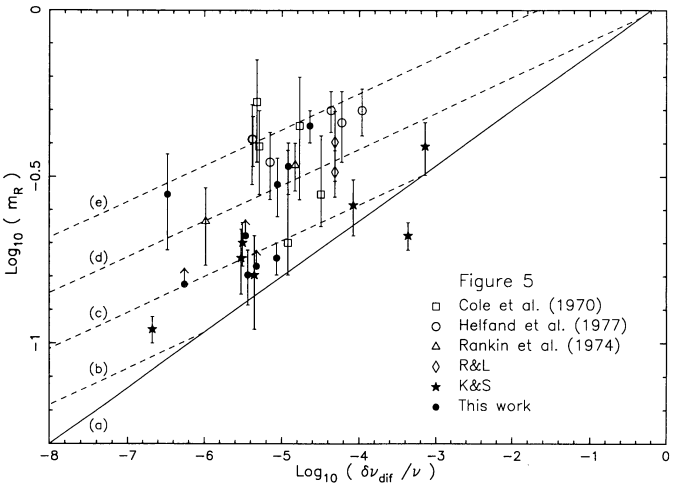

FIG. 5.—Refractive scintillation m_r index vs. $\delta\nu_d/\nu$ (see Appendix B for theory). The data points for the pulsar observations described here and for the observations of more distant pulsars at 610 MHz by K&S are plotted as filled symbols. Open symbols give previously published values. Points with arrows are lower bounds. The lines show the expected behavior for a Kolmogorov spectrum with inner scales of: (*a*) 0, (*b*) 10^7 m, (*c*) 10^8 m, (*d*) 10^9 m, and (*e*) 10^{10} m.

in Figure 5. The lines have a logarithmic slope of 0.108, which has the effect of decreasing m_r over the previous plots at a given inner scale. An overall comparison with the data suggests an inner scale of 10^8 or 10^9 m. The model with an inner scale cutoff to a Kolmogorov spectrum is, of course, only one of many possible models. Another would be a simple power law with an exponent slightly steeper than the Kolmogorov value. The solid line in Figure 5 would have a slope $1 - \alpha/2$, for a wavenumber exponent $-\alpha - 2$. Such a line passing through the higher values of m_r would have $\alpha \sim 1.8$. This model does not have the physical basis of the Kolmogorov model with an inner scale, and so we do not consider it further. In a more general description, we can discuss any model spectrum that has a ratio of power density between the refractive scales and the diffractive scales, that is greater than the Kolmogorov ratio by a factor of about 4:1. Such a spectrum would be consistent with the m_r observations that lie about a factor of 2 above the Kolmogorov line; though this ratio is still less than that for $\alpha = 2$.

There is a weak distance dependence in (B7) ignored in Figure 5. In order to include this dependence we also computed the theoretical m_r for inner scales of 0, 10^7, 10^8, 10^9 m, for the actual distances of all of the published measurements of m_r that include an error. The differences between measurement and the four theoretical values were each normalized by the published rms error and used to compute a χ^2 (sum of squared normalized differences from theory) and also to compute an rms difference without normalization. These are tabulated in Table 3 for all 26 measurements and also for the 13 measurements from our 74 MHz and the 610 MHz measurements of K&S. The minimum χ^2 corresponds to an inner scale of 10^8 m, which is also the value giving the smallest unweighted rms for the second set. When all the data are included 10^8 m still gives the smallest χ^2, but 10^9 m gives a smaller rms, due particularly to several large values of m_r measured by Helfand et al. (1977). The minimum χ^2 exceeds its expected value by 14 and 9 standard deviations, respectively for the two data sets. Thus the observations are not statistically homogeneous. There is more

TABLE 3

χ^2 AND RESIDUAL ERRORS VERSUS INNER SCALE

DATA SET	NUMBER OF OBSERVATIONS	METHOD	INNER SCALE (m)			
			0	10^7	10^8	10^9
1–6	26	χ^2	182	177	123	303
		rms	0.19	0.19	0.16	0.11
5, 6	13	χ^2	85	80	58	287
		rms	0.12	0.12	0.09	0.10

NOTES.—Data set 1: Cole et al. 1970 via R&L. Data set 2: Helfand et al. 1977 via R&L. Data set 3: Rankin et al. 1974. Data set 4: R&L. Data set 5: K&S. Data set 6: results of present paper.

scatter in the data than is compatible with a single value of inner scale.

We note that most of the high values of m_r are from nearby high-latitude objects. This suggests that the inner scale may be larger for these pulsars. Conversely, a smaller inner scale is suggested for the more distant objects, for which the Kolmogorov theory seems adequate. Many of these distant pulsars show enhanced scattering, suggesting that small inner scale may be associated with an enhanced level of plasma turbulence. This is an entirely reasonable supposition in that a locally increased turbulent power would push the inertial range to smaller scales, under the assumption that, as in viscous damping, the dissipation rate is inversely related to dissipation scale. Note, however, that our best determined measurement (PSR 1133+16) is a nearby pulsar that does not indicate a high level of scintillation, suggesting an inner scale smaller than about 10^7 m. Differing values of the inner scale have been inferred by different authors. In their original proposal, Coles et al. (1987) proposed a value of about 10^9 m. Using VLBI observations, Spangler & Gwinn (1990) inferred a value of 10^6 m. It is interesting that many of the VLBI measurements were made on sources with very strongly enhanced scattering, for which according to the hypothesis above there would be a smaller inner scale. We suggest this as a possible reconciliation of inner scale values that differ by a factor of over 1000. It is difficult to push this idea further since we do not know the relation between the density spectrum and the velocity spectrum. However, if hydrodynamics applied and we used the density spectrum to estimate the velocity spectrum, the six orders of magnitude range observed in strength of the density spectrum, would correspond only two orders of magnitude change in the viscous dissipation scale.

4.2. *Refractive Scintillation Time Scale*

We now turn to the time scale results. In all cases the observations are consistent with time scales considerably shorter than the Kolmogorov prediction. The measured slope of the structure function is largely determined by the time scale, since the range in m_r^2 is not very great, but sometimes the slope responds to the presence of a process with a time scale shorter than that computed by finding the lag at 50% of saturation. The measured slopes are all greater than the predictions, by factors that range from 1.5 to 150. For pulsars PSR 0329+54 and PSR 1919+21 our data show some weak scintillation over scales longer than 100 days, consistent with the predicted RISS times of 313 and 113 days, respectively. Here the slopes are useful and exceed the predictions by factors of 4 and 2, respectively. For PSR 0809+74 we find evidence for a time scale in the range 4–16 days, substantially shorter than the predicted RISS time of 105 days (or possibly as short as 47 days). For PSR 0834+06 we have weak evidence for a time scale less than or equal to 40 days, compared with a predicted value of 120 days. For PSR 1133+16 we estimate 9 ± 3 days, again substantially shorter than the predicted value of 18 days. For PSR 1508+55, we find a time scale (47 ± 37 days) which, though poorly constrained, is comparable to the smallest of the predicted values (55 days), but the structure function has a much larger slope than predicted. Similarly for PSR 1237+25 we estimate a time scale less than or equal to 40 days, consistent with the 40 day prediction. For PSR 0950+08 the data give a time scale 3 ± 1.5 days, which is shorter than the expected value by a factor of 20–50, depending on velocity uncertainties. It is not clear whether the results for PSR 0950+08 are part of the same trend for the predicted RISS time scales to overestimate the observed values, or whether it represents a special case. It was argued that changing Faraday rotation in the ionosphere causes the day-to-day variance, but that it could not also cause its 3 day variations. It is interesting that this pulsar with the largest and fastest amplitude variations is closest to the Earth and has the slowest velocity.

It is notable that in their conclusions K&S reported time scales both above and below their theoretical predictions for the 14 pulsars that they observed. The theory for the RISS time scale that we have used is very simple, namely that $\tau_r \approx 0.5Z\theta_o/V$, where Z is the pulsar distance and θ_o is the angular radius of the scattered image and V is the velocity. In equation (3) and (3a) we relate τ_r to δv_d. K&S used a similar relation in their equation (3), but included a constant K that in our analysis equals 3.1, whereas they assumed a value 1.0. Using $K = 3.1$ their measured time scales would also be shorter than or similar to the predictions. Thus the two sets of observations agree on this point, and the discrepancy is not confined to the nearby pulsars. It is still necessary to address the question of the correct theory for the time scale. K&S do not attempt to justify their choice of $K = 1.0$ on theoretical grounds; our value is based on approximate analysis of a simple uniform distribution of scattering material (Coles et al. 1987). There is a need for a more definitive theory but we suggest that $K = 3.1$ has some justification. We note that the time scale also depends linearly on the assumed distance and inversely on the assumed velocity. The distances used here are as tabulated in Cordes (1986) and any revisions of distance scale would change our conclusions. We used the proper motion velocities where possible, whereas K&S used the "scintillation velocities" from Cordes (1986). These are consistently slower for all of our pulsars (V_{iss}/V_{pm} ranging from 0.25 to 1.2, mean 0.5). Clearly the predicted time scales would be lengthened if we used the scintillation velocities. It is reasonable to suppose that the scintillation velocities are the most appropriate, since the proper motion would be insensitive to any plasma motion of the ISM. Thus in some sense the discrepancy is worse than given in Table 2. We note that the discrepancy might be due to a failure of the "frozen pattern hypothesis," that we use in mapping spatial scales into time scales. If this were the case we would need to explain why random plasma motion was more important for the large scales than for the small scales.

As in equation (3) the predicted τ_r also depends on the inverse square root of the measured δv_d, and so provides a source of uncertainty in the predictions. The stability of the estimated δv_d has not been studied extensively. In general variations from one report to another are within a factor of 2, with some exceptional pulsars standing out with variations by

as much as a factor of 8. There is an interesting point that the influence of refraction on diffractive scintillations is to cause diffractive features to drift in frequency and that this reduces the effective decorrelation bandwidth (Hewish et al. 1985). Thus the effect of refraction is that the observed decorrelation bandwidth typically underestimates the true $\delta\nu_d$ and so biases the expected time scale upwards. If the variability is typically a factor of 2 as suggested above, the mean value will be low by about a factor of 1.4 and this would bias τ_r high by 20%. This is insufficient to explain the discrepancy, though it does go in the right direction. A procedure for combating this bias would be to use the largest value of $\delta\nu_d$ available from the literature. The practical difficulty is that differing methods of estimating $\delta\nu_d$ by different observers also add uncertainty; we used the uniform set of Cordes (1986) for this reason. The pulsars PSR 0809+74 and PSR 1508+55 show exceptionally large variations in decorrelation bandwidth and, as footnoted in Table 2, lead to reduced predictions for τ_r; in the latter case this removes the discrepancy. PSR 0834+06 is also very variable; Roberts & Ables (1982), reported a factor of 5 change over 1 yr. However, in comparing the predicted τ_r we find that the values based on Cordes observations lies between the two extremes derived from the observations of Roberts and Ables, and that the smallest value of τ_r is 75 days compared to the observed value of 19 ± 16 days. Thus even including the pulsars with exceptionally variable decorrelation bandwidth, the puzzling time scale discrepancy remains.

The other important unknown in this problem is the true distribution of scattering material along each line of sight. In the formulae used above a uniform distribution is assumed, and where necessary it is represented by a single screen midway between pulsar and observer. A localized screen asymmetrically located is an alternative model, particularly for sources with enhanced scattering. In Appendix C, we give formulae for τ_r in terms of an observed $\delta\nu_d$, a distance Z_p from pulsar to screen and a distance Z_o from screen to observer. There are three limiting cases of interest.

$$\text{If } Z_p = Z_o\,; \quad \tau_r \approx A(Z_p + Z_o)^{0.5}/|V_p + V_o|$$
$$\text{If } Z_p \ll Z_o\,; \quad \tau_r \approx AZ_p^{0.5}/V_p$$
$$\text{If } Z_p \gg Z_o\,; \quad \tau_r \approx AZ_o^{0.5}/V_o\,,$$
$$\text{where } A = \sqrt{c/(4\pi\delta\nu_d)}\,.$$

Thus one possible explanation for the shorter than expected time scales is that the medium is far from uniform and is dominated by scattering in a single screen, either very near the pulsar or very near the Earth. A reduction by a factor of 5 would require a 25:1 ratio of the two screen distances. It is also necessary to consider whether an asymmetrically placed screen would alter the rms level m_r of the scintillations. We have considered this question and conclude that equation (B2) correctly gives the value of m_r in terms of the observed $\delta\nu_d/\nu$. This conclusion applies for a zero inner scale, but it is clear that an inner scale would introduce only a very weak distance dependence, similar to that in equation (B7). Thus we can consider the screen location as a free parameter in an attempt to match the time scale results. A "screen" location near the pulsar seems more likely and reduces the time scale more effectively since pulsar velocities are often high. A second possible explanation lies in the effect of the inner scale on τ_r. It is known (e.g., Goodman et al. 1987) that, as the inner scale is increased toward the scale of the scattering disk, there is power added at scales intermediate between the refractive and diffractive scales. Current analyses of this phenomenon suggests that it is not a large effect until the inner scale is nearly as large as the scattering disk, requiring an inner scale several orders of magnitude larger than that suggested above. However, more theoretical work is needed with a consistent analysis of the accompanying $\delta\nu_d$. A third possibility is that the method of estimating the time scale gives a systematically low value, when compared with the theoretical expression. However, an evaluation of this possibility requires a full simulation, that is beyond the present study. The factor of 2 or more disagreement with theory has a parallel consequence for the time scale of RISS expected of extragalactic radio sources. The discrepancy is in the same sense and of a similar magnitude to that found by Spangler et al. (1991), in their study of RISS from extragalactic radio sources that exhibit low-frequency variability. A common explanation seems likely but eludes us at present.

We have confined our studies to parameterizing the structure functions, rather than examining their shape. The reason is twofold. First there are likely biases at small time lags due to errors in the noise subtraction and the gain correction. Second there are substantial statistical errors in our data, in which the observing span is commonly not very long compared to τ_r. However, in many cases the slope near the origin is reasonably well determined and as noted gives values much in excess of the predictions. There are a number of points concerning the theory for the slope, that require comment. The theoretical expression is taken to be $2m_r^2/\tau_r$, which is only correct for a structure function that is linear at small lags. This formally excludes structure functions in the presence of an inner scale; they become quadratic and have an asymptotically zero slope. However, our sample interval of 1 day corresponds to a spatial sample interval of 4×10^9 m or greater, which is too coarse to detect curvature in the structure function on the small inner scales that are proposed. Another point concerns the structure function when the inner scale becomes comparable to the refractive scale. As mentioned above this condition gives extra small-scale power, that could steepen the slope. Again for the inner scales proposed, we estimate this to be unimportant. The final point about the shape is that it is strongly influenced by the distribution of scattering strength along the line of sight. Only for the uniform medium model is the structure function approximately linear. For a screen model it should be quadratic; indeed Coles (1988) showed that an extended medium that lacks as little as 10% of the line of sight near the observer gives rise to a structure function that is noticeably quadratic. Our data appear to be much nearer to linear than quadratic and so are in disagreement with a single screen model, which is the most obvious solution to the time scale problem discussed above. In their analysis K&S found that their structure functions depend on lag to an exponent in the range 1.0 and 1.5. Thus their shapes are nearer to linear than to quadratic and so support the uniform medium model and reinforce this disagreement. A possible resolution might be the superposition of an extended medium continuous to near the Earth, with a screen having much enhanced scattering. Such a scattering distribution might also give fluctuations that are not "frozen" over the refractive time scales. However, it is beyond the scope of this paper to pursue these ideas.

4.3. *Conclusions*

We end by stating our main conclusions. The 74 MHz observations show an RISS modulation index, that is enhanced over that for a Kolmogorov spectrum particularly for several

nearby pulsars. Such an enhancement suggests the influence of an inner scale cutoff to the wavenumber spectrum at about 10^8 m. This could be reconciled with 610 MHz observations (by K&S) of more distant heavily scattered pulsars that are only slightly above the Kolmogorov model, if the inner scale were inversely related to the local strength of scattering. This hypothesis might even explain the VLBI estimates of inner scale near 10^6 m. The observed time scales of RISS are systematically less than those expected on a simple model with uniform distribution of scattering material, typically by a factor of 2 or more. Several explanations have been proposed but none seems entirely satisfactory. These conclusions point to the inadequacy of the simple models for RISS in quantitative explanations of the time scales of radio source variations. Thus more observations are needed to tighten the description of the RISS phenomena (particularly for PSR 0950+08). A reevaluation of the theory with an inner scale and a more realistic distribution of both scattering strength and velocity is also clearly needed.

We gratefully acknowledge a grant (CS-14-89) from the California Space Institute that provided one year of support for the observations.

APPENDIX A

ESTIMATION ERRORS IN PULSE AMPLITUDES

The estimated errors in the daily pulse strength δP_{jp} and in the system gain δG_{jp} (listed as "nvar" and "gvar" respectively, in Table A1) are combined to give the error δS_{jp} in the corrected daily pulse strength. However, there are several sources of variation which are not accounted for in this estimate. Evidently the error in the system gain estimate is included, as are any pulse variations that occur over times shorter than the length of the pulse period. These include rapid intrinsic pulse variations (subpulses and micropulses), interplanetary scintillation and system noise. The modulations not accounted for include: longer intrinsic (pulse to pulse and day to day) fluctuations, ionospheric scintillations, varying faraday rotation of the linearly polarized pulsar signal by the ionosphere, and residual diffractive interstellar scintillation. In calculating the contribution to the variance from each of these, we note our integration over 20–40 minutes reduces the effect of all of these except for intrinsic day to day variations and the effect of changing faraday rotation. Each process is discussed below and in Table A1 we list its net contribution to the normalized pulse amplitude variance.

System Noise.—In integrating a pulsar of period P for T seconds, we coherently average T/P pulses, forming a daily pulse profile, which is fitted with a template. The fitted amplitude has an error due to residual noise in the profile. The signal I and rms noise N in this case are given by

$$I = 0.5\, G_t \frac{P}{\tau_p} S_{\rm av} A_e B\,, \tag{A1}$$

$$N = \frac{G_t k T_s B}{\sqrt{B\tau_p}} \times \sqrt{\frac{P}{T}}\,, \tag{A2}$$

where G_t is the total gain from RF to post-detection, $S_{\rm av}$ is the time-averaged flux at 74 MHz, A_e is the effective area of the antenna, B is the observing bandwidth, T_s is the system noise temperature, τ_p is the width of the profile template and k is the Boltzmann constant. This expression ignores the noise in the off-pulse part of the profile. The rms noise normalized by the average pulse amplitude is then

$$\frac{N}{I} = \frac{2kT_s}{S_{\rm av} A_e \sqrt{BTP/\tau_p}}\,. \tag{A3}$$

In most of our observations the observed pulse width τ_p was dominated by dispersion and so was proportional to the receiver bandwidth B; in such cases one can see that the signal-to-noise ratio is then nominally independent of bandwidth. Initially we

TABLE A1

ESTIMATION OF THE "NOISE" VARIANCES (HALF THE UNIT-LAG STEP IN THE STRUCTURE FUNCTIONS)

Pulsar	nvar	fvar	invar	scvar	dsvar	gvar	tvar	mvar
P0329+54.....	3.4×10^{-3}	4.0×10^{-5}	3.0×10^{-4}	2.1×10^{-5}	1.6×10^{-5}	7.2×10^{-3}	1.1×10^{-2}	1.1×10^{-2}
P0809+74.....	6.6×10^{-3}	6.5×10^{-4}	1.0×10^{-3}	4.2×10^{-5}	1.6×10^{-5}	7.8×10^{-3}	1.6×10^{-2}	8.0×10^{-2}
P0823+26.....	9.5×10^{-3}	1.7×10^{-2}	4.4×10^{-4}	4.2×10^{-5}	1.6×10^{-5}	7.5×10^{-3}	3.4×10^{-2}	2.8×10^{-2}
P0834+06.....	1.4×10^{-3}	4.7×10^{-4}	1.1×10^{-3}	4.2×10^{-5}	1.6×10^{-5}	8.4×10^{-3}	1.1×10^{-2}	1.4×10^{-2}
P0950+08.....	3.1×10^{-3}	4.4×10^{-1}	1.1×10^{-4}	2.1×10^{-5}	1.6×10^{-5}	8.8×10^{-3}	4.5×10^{-1}	5.1×10^{-1}
P1133+16.....	5.6×10^{-4}	3.1×10^{-2}	4.9×10^{-4}	2.1×10^{-5}	1.6×10^{-5}	9.8×10^{-3}	4.2×10^{-2}	1.4×10^{-2}
P1237+25.....	1.1×10^{-2}	5.1×10^{-2}	5.8×10^{-4}	2.1×10^{-5}	1.6×10^{-5}	9.4×10^{-3}	7.2×10^{-2}	6.5×10^{-2}
P1508+55.....	2.6×10^{-3}	1.6×10^{-4}	2.1×10^{-4}	2.1×10^{-5}	1.6×10^{-5}	9.8×10^{-3}	1.3×10^{-2}	1.1×10^{-2}
P1919+21.....	8.5×10^{-4}	7.2×10^{-5}	1.1×10^{-3}	4.2×10^{-5}	1.6×10^{-5}	7.7×10^{-3}	9.8×10^{-3}	1.9×10^{-2}

NOTES.—nvar is variance due to system noise; fvar is variance due to random ionospheric Faraday Rotation; invar is variance due to intrinsic pulsar fluctuations; scvar is variance due to ionospheric scintillation; dsvar is variance due to diffractive scintillation leakage; gvar is variance due to errors in gain correction; tvar is the predicted total variance; mvar is variance as measured from unit lag step in structure functions.

estimated the expected pulsar fluxes at 74 MHz from the published fluxes at 400 MHz and the spectral index between 400 and 1400 MHz. With $T_s = 1000$ K, the calculations predicted signal to noise ratios in the range 200 to 20,000 for the pulsars. In fact T_s is dominated by Galactic noise and is substantially larger near the Galactic plane. If the pulsar spectrum has a low-frequency turnover between 74 and 400 MHz, it would also reduce the signal. For example, this is certainly true for P0329+54—whose spectrum is known to turnover at about 100 MHz—for which the observed signal was not as great as predicted. In fact one of the results of our observations is an estimate of the average flux at 74 MHz for each of the pulsars. See Table 1. As discussed below, the signal-to-noise ratios as observed are determined by the various contributions to pulse fluctuation rather than by system noise, except in the cases of PSR 0823+26 and PSR 1237+25.

Rapid Intrinsic Variations.—Many pulsars are known to exhibit large—as much as 100%—intrinsic fluctuations from one pulse to the next. This effect can bias the daily pulse strength estimate if an insufficient number of pulses are averaged to obtain the daily pulse profile. For our observations, a typical averaging period is 30 minutes. Using a typical pulsar period of 1 s, gives an average over 1800 pulses. This would reduce 100% pulse-to-pulse modulation to $100/\sqrt{1800} = 2.4\%$ modulation. This is a small level of fluctuation. The value for each pulsar is entered in the column "invar" in Table A1.

Ionospheric Scintillations.—Ionospheric scintillations, which occur on time scales shorter than the averaging period, can also bias the daily pulse strength estimate. For these, if we take 50% as a typical large modulation index and 10 s as a typical time scale, then a 30 minute observation includes 180 such independent fluctuations, reducing the observed modulation index to 3.8%. Again this is a small level of fluctuation. The individual values are entered under column "scvar" in Table A1.

Ionospheric Faraday Rotation.—The Fallbrook antenna is sensitive to linearly polarized radiation with the electric field in the local north-south direction. Since a significant fraction of radiation from most pulsars is linearly polarized, apparent variations in pulsar flux will occur as the angle of polarization changes. The most serious contribution is from changes in Faraday rotation as the total electron content in the Earth's ionosphere changes over times of hours to days. If I_x is the ratio of apparent intensity in x-polarization to its value averaged over all angles of polarization and m_p is the fraction of the total intensity in the linearly polarized component, then neglecting circular polarization we have

$$I_x(f, t) = (1 - m_p) + 2m_p \cos^2 [\theta_a(t) - \phi_t(f)] . \quad \text{(A4)}$$

Here $\theta_a(t)$ is the offset angle between the direction of the antenna and the direction of the linearly polarized component. For most pulsars it is found to vary with time across the pulse in an approximately linear fashion, i.e., $\theta_a(t) = \theta_{a0} + Kt$. The quantity $\phi_t(f)$ is the total Faraday rotation angle of the linearly polarized component, given by

$$\phi_t(f) = \lambda^2[(\mathrm{RM})_{\mathrm{ism}} + (\mathrm{RM})_{\mathrm{ion}}] , \quad \text{(A5)}$$

where $(\mathrm{RM})_{\mathrm{ism}}$ and $(\mathrm{RM})_{\mathrm{ion}}$ are the contributions to the rotation measure from the interstellar medium and the ionosphere. Integration of equation (A4) over the observing bandwidth and the pulse width gives the total observed pulse strength for any single day's observation. Since the bandwidth B is much smaller than the center frequency f_o, the variation of ϕ_t over the band can be treated as approximately linear. Under this assumption, the following normalized expression for the apparent pulse flux results

$$S_x = 1 + m_p \,\mathrm{sinc}\,(2\phi_{t0} B/f_o)\,\mathrm{sinc}\,(\mathrm{K}\tau_p)\cos[2(\theta_{a0} - \phi_{t0})] . \quad \text{(A6)}$$

Here ϕ_{t0} is the total Faraday rotation at the center of the band, τ_p is the pulse width, θ_{a0} is the offset angle at the center of the pulse and $\mathrm{sinc}\,(x) = \sin(x)/x$.

For typical values of magnetic field and electron density in the ionosphere, it can be shown that even a 5% fluctuation in the electron content in the ionosphere can cause a change of Faraday rotation of more than 1 rad at 74 MHz. Thus under the worst case conditions the cosine term in equation (A6) will vary through its maximum range of -1 to $+1$. This will lead to a worst case apparent modulation index of

$$m_{fr} = 0.707 m_p \,|\,\mathrm{sinc}\,(2\phi_{t0} B/f_o)\,|\,|\,\mathrm{sinc}\,(K\tau_p)\,| . \quad \text{(A7)}$$

The values of m_{fr} are tabulated in Table A2 together with the parameters RM, m_p, ϕ_{t0}, $K\tau_p$. They come from the literature (Taylor & Manchester 1975; Morris, Graham, & Seiber 1981; Schwarz & Morris 1971; Lyne & Manchester 1988) and are extrapolated to a frequency of 74 MHz, but we note that they are somewhat uncertain. The rotation measures are those tabulated in the literature, which typically include an ionospheric contribution of about 0.6 rad m^{-2}. This value is quite uncertain and no attempt was made to

TABLE A2

APPARENT INTENSITY MODULATION OF PULSARS DUE TO VARIABLE FARADAY ROTATION

Pulsar	RM (rad m^{-2})	m_p (74 MHz)	ϕ_{t0} (rad)	$K\tau_p$	m_{fr}
PSR 0329+54.....	−63.7	0.2	−1052	90°	6.3×10^{-3}
PSR 0809+74.....	−11.7	0.2	−193	30	2.5×10^{-2}
PSR 0823+26.....	5.9	0.3	98	60	1.3×10^{-1}
PSR 0834+06.....	23.6	0.3	390	90	2.2×10^{-2}
PSR 0950+08.....	1.35	1.0	22	35	6.6×10^{-1}
PSR 1133+16.....	3.9	0.5	64	100	1.75×10^{-1}
PSR 1237+25.....	0.33	0.5	5.4	90	2.2×10^{-1}
PSR 1508+55.....	0.8	0.3	13	180	1.2×10^{-2}
PSR 1919+21.....	16.5	0.15	273	100	8.5×10^{-3}

monitor the ionospheric term, since even a 5% error in it will change the polarization angle by 1 rad. Thus the day-to-day pulsar fluctuations contain an ionospheric term with an rms magnitude given by m_{fr}. The square of this gives a contribution to the observed variance tabulated as "fvar" in Table A1. Of all the effects discussed in this section, Faraday rotation is the most critical.

In view of the dominance of the apparent variations discussed above, we also ask whether they could cause a variation over times longer than 1 day, in particular whether they might be responsible for the large amplitude 3 day variations in PSR 0950+08. For this pulsar equation (A6) becomes $S_x = 1 + \cos[\Phi(t)]$, where $\Phi = [2(\theta_{a0} - \phi_{t0})]$ is twice the angle between the average pulsar polarization and the antenna orientation. Thus the question to be answered is what is the temporal correlation function for S_x?

$$C(\tau) = \langle \Delta S_x(t)\, \Delta S_x(t+\tau) \rangle \qquad \text{where} \qquad \Delta S_x(t) = \cos(\Phi) - \langle \cos(\Phi) \rangle \,. \tag{A8}$$

We can evaluate $C(\tau)$, if $\Phi = \Phi_o + \delta\Phi$ and $\delta\Phi$ is a zero mean Gaussian random variable. The result is simple, if σ_Φ the rms variation in $\delta\Phi$ is many radians

$$C(\tau) = 0.5 \exp[-0.5 D_\Phi(\tau)] \qquad \text{where} \qquad D_\Phi(\tau) = \langle [\Phi(t) - \Phi(t+\tau)]^2 \rangle \,. \tag{A9}$$

The error involves terms of order $\exp[-\sigma_\Phi^2]$. Thus (A9) will be accurate to within 2% if $\sigma_\Phi > 2$. So we need to know the statistics of Φ. For the present purposes we refer to the work of Schwarz & Morris (1971), in which they measured the variation in Φ at 150 MHz for PSR 0950+08. Their Figure 3 shows $\Phi/2$ varying linearly over 45 minutes at a rate of 90° per hr. This scales to 12 rad per hr at 74 MHz. We suggest that this provides reasonable evidence that σ_Φ is much larger than a radian, justifying equation (A9). Hence we can use equation (A9) to consider what apparent flux variations would be seen on times longer than 1 day. Setting $\tau = 1$ day, we find a residual variance $0.5 \exp[-0.5 D_\Phi(\tau = 1 \text{ day})]$. We do not know $D_\Phi(\tau = 1 \text{ day})$, but it is hard to imagine that it is less than 9 rad^2, if 12 rad per hr is at all typical. The corresponding residual variance is then much less than 1%. This provides the argument that the 3 day variations of PSR 0950+08 are not caused by variable ionospheric polarization rotation.

Diffractive Scintillation.—Diffractive scintillation changes randomly with time and frequency and so can modulate the daily pulse strength estimate, depending on the number of independent diffractive scintles present in a single day's data. This number is given by

$$N = [B/v_d][T/\tau_d] \,, \tag{A10}$$

where B is the observation bandwidth, T is the total observation time, v_d and τ_d are the decorrelation bandwidth and time scale, respectively, of the diffractive scintillations. For typical values of the scattering parameters and a pulsar at a distance of 500 pc moving with a relative velocity of 100 km s^{-1}, $v_d = 270$ Hz and $\tau_d = 50$ s. Thus, for a bandwidth of 500 kHz and a 30 minute observation, $N = 65{,}800$ and this would reduce a 100% diffractive scintillation to 0.4%. This is again a very small effect and is tabulated under "dsvar" in Table A1.

Since the time scales for all the above process are less than a day, they contribute to the unit lag step in the structure function for the corrected pulse strength. Table A1 lists the expected contributions to the variance in the pulse strength. Wherever exact calculations are not possible, typical worst case numbers have been used. The sum of these contributions is "tvar" in Table A1; it is to be compared with the measured variance "mvar," estimated as one-half the value of D_S at a lag of 1 day. That these are of the same order of magnitude gives us confidence that in general we understand the sources of "noise." However, there are cases where tvar exceeds mvar and there are sufficient uncertainties in the individual pulsar parameters, that the estimate tvar cannot be used to correct D_S for the unit lag step. Consequently we have simply subtracted the measured value of D_S at a lag of 1 day.

APPENDIX B

REFRACTIVE SCINTILLATION INDEX

In the theoretical analysis of the refractive scintillation index m_r for emission from a point source like a pulsar, the following parameters have to be specified (in reference to the model for the wavenumber spectrum of electron density in equation (1) of Coles et al. 1987): $C_N^2(z)$ is the distribution of scattering strength with distance z (the two standard models are a uniform distribution along the line of sight or a localized "screen"); $-\alpha - 2$ is the exponent of the power-law part of the wavenumber spectrum, which we take to be the Kolmogorov value of $-11/3$; s_i is the inner scale; Z is the pulsar distance; λ is the observing wavelength.

A simple physical model for the turbulence distribution is that C_N^2 is independent of position in the Galaxy. However, this is far from what is observed; rather there is a wide range in this quantity over differing lines of sight. Thus the method which we use to estimate these quantities is to rely on the observed δv_d, the frequency difference at which the correlation of diffractive scintillations falls to 0.5. This gives a measure of the level of scattering on each line of sight and is related to the scattering parameters by

$$\frac{\delta v_d}{2v} = f\left[\frac{s_0}{r_f}\right]^2, \qquad \text{where} \qquad r_f = \left[\frac{Z\lambda}{2\pi}\right]^{1/2} . \tag{B1}$$

Here s_0 is the field coherence scale, at which the structure function of phase equals one, and f is a constant that comes from the specification of 0.5 in defining δv_d. We use $f = 1.0$, noting that it changes between a screen and uniform model, and Cordes et al. (1986) use $f = 0.76$; since it affects the results only to a power of 0.166, the differences are slight. The scale s_0 is related to the same quantities listed above and in turn can be related to m_r. With a uniform scattering distribution the results are

$$m_r \approx 1.21[s_0/r_f]^{1/3} \approx 1.08[\delta v_d/v]^{1/6}, \qquad \text{where} \qquad s_i < s_0 \tag{B2}$$

$$m_r \approx 1.21[s_0/r_f]^{1/6}[s_i/r_f]^{1/6}, \qquad \text{where} \qquad s_i > s_0 \,. \tag{B3}$$

In order to predict m_r in terms of $\delta v_d/v$, we need (B1) and also a relation to r_f. The same question was addressed by R&L in their Figure 4. Unfortunately, there is an error in their analysis which is corrected as follows.

For an extended uniform distribution $\delta v_d/v$ depends on Z and λ as

$$\delta v_d/v \propto \lambda^{-3.4} Z^{-2.2} , \tag{B4}$$

and hence

$$r_f = r_{fo}[\lambda/\lambda_o \, Z/Z_o]^{1/2} \tag{B5}$$

$$r_f = r_{fo}\left[\frac{Z}{Z_o}\right]^{1.2/6.8}\left[\frac{\delta v_{do}/v_o}{\delta v_d/v}\right]^{1/6.8} . \tag{B6}$$

This is substituted into (B3) for $s_i > s_0$ to finally give

$$m_r = 1.14[\delta v_d/v]^{0.1078}[s_i/r_{fo}]^{1/6}[\delta v_{do}/v_o]^{-0.0245}[Z/Z_o]^{-0.0294} . \tag{B7}$$

This result expresses m_r in terms of $\delta v_d/v$ and standard values r_{fo} and $\delta v_{do}/v_o$ at Z_o and λ_o. In our analysis we have taken $Z_o = 1$ kpc, $\lambda_o = 1$ m, and $\delta v_{do}/v_o = 10^{-4}$. The latter value seems nearer to the typical observational results than 10^{-3}, used by R&L. In comparing observations of m_r with theory we plot them against $\delta v_d/v$ as scaled to the same frequency as the observed m_r, but we ignore the dependence on distance Z in (B7).

APPENDIX C

REFRACTIVE TIME SCALE

Equation (3) for τ_r comes from an approximate analysis of the scattering in an extended medium, in which V is the relative velocity of the refractive pattern and the observer, δv_d is the measured diffractive scintillation bandwidth and Z is the distance to the pulsar. Consider now scattering from a screen localized between the pulsar and observer. Let Z_p be the distance from pulsar to screen and Z_o be from screen to observer. Let the velocity of the pulsar be $\boldsymbol{V}_p$ and that of the observer be $\boldsymbol{V}_o$, taken with respect to the screen. Then using the analysis of Appendix B from Rickett (1986), we find

$$\tau_r \approx \frac{0.5(Z_o + Z_p)\theta_{\rm app}}{|\boldsymbol{V}_p + \boldsymbol{V}_o(Z_p/Z_o)|} .$$

Here $\theta_{\rm app}$ is the apparent angular radius of the scattering disk seen by the observer. This can be related to the pulse broadening time δt as

$$\delta t = \frac{(Z_o + Z_p)\theta_{\rm app}^2}{2c}\frac{Z_o}{Z_p} .$$

Then relating this to the diffractive bandwidth δv_d by $\delta t \approx (2\pi\delta v_d)^{-1}$, we obtain

$$\tau_r \approx 0.5\sqrt{\frac{cZ_p(Z_o + Z_p)}{\pi\delta v_d Z_o}}\frac{1}{|\boldsymbol{V}_p + \boldsymbol{V}_o(Z_p/Z_o)|}$$

If velocities were referred to some other standard of rest and the screen also had motion with respect to that standard, $\boldsymbol{V}_p$ would be replaced by the velocity difference between pulsar and screen and a similar replacement for the observer velocity. In modeling the RISS of the pulsars, we know the earth's velocity with respect to the Sun and the proper motion measurements give pulsar velocity also with respect to the Sun. We do not know the screen velocity and have set this to zero, but it is evidently one of the weaknesses of the model.

REFERENCES

Armstrong, J. W., & Rickett, B. J. 1981, MNRAS, 194, 623
Blandford, R. D., & Narayan, R. 1985, MNRAS, 213, 591
Cole, T. W., Hesse, H. K., & Page, C. G. 1970, Nature, 225, 712
Coles, W. A. 1988, in AIP Conf. Proc. No. 174, Radiowave Scattering in the Interstellar Medium, (NY: AIP), 163
Coles, W. A., Frehlich, R. G., Rickett, B. J., & Codona, J. L. 1987, ApJ, 315, 666
Coles, W. A., Liu, W., Harmon, J. K., & Martin, C. L. 1991, J. Geophys. Res., 96, 1745
Cordes, J. M. 1986, ApJ, 311, 183
Cordes, J. M., Weisberg, J. M., & Boriakoff, V. 1985, ApJ, 288, 221
Goodman, J. J., & Narayan, R. 1985, MNRAS, 214, 519
Goodman, J. J., Romani, R. W., Blandford, R. D., & Narayan, R. 1987, MNRAS, 229, 73
Helfand, D. J., Fowler, L. A., & Kuhlman, J. V. 1977, AJ, 82, 701
Hewish, A., Wolszczan, A., & Graham, D. A. 1985, MNRAS, 213, 167
Kaspi, V. M., & Stinebring, D. R. 1992, ApJ, 392, 530 (K&S)
Lyne, A. G., Anderson, B., & Salter, M. J. 1982, MNRAS, 201, 503
Lyne, A. G., & Manchester, R. N. 1988, MNRAS, 234, 477
Manchester, R. N., & Taylor, J. H. 1981, AJ, 86, 1953
Manchester, R. N., Taylor, J. H., & Huguenin, G. R. 1975, ApJ, 196, 83
Morris, D., Graham, D. A., & Sieber, W. 1981, A&A, 100, 107
Rankin, J. M., Payne, R. R., & Campbell, D. B. 1974, ApJ, 193, L71
Rickett, B. J. 1970, MNRAS, 150, 67
———. 1986, ApJ, 307, 564
———. 1990, ARA&A, 28, 561
Rickett, B. J., Coles, W. A., & Bourgois, G. 1984, A&A, 134, 390
Rickett, B. J., & Lyne, A. G. 1990, MNRAS, 244, 68 (R&L)
Roberts, J. A., & Ables, J. G. 1982, MNRAS, 201, 1119
Schwarz, U. J., & Morris, D. 1971, Astrophys. Lett., 7, 185
Sieber, W. 1982, A&A, 113, 311
Spangler, S. R., Eastman, W. A., Gregorini, L., Mantovani, F., & Padrielli, L. 1991, A&A, preprint
Spangler, S. R., & Gwinn, C. 1990, ApJ, 353, L29
Stinebring, D., & Condon, J. J. 1990, ApJ, 352, 207
Taylor, J. H., & Manchester, R. N. 1975, AJ, 80, 794

Note added in proof.—In a recent preprint, J. A. Phillips and A. Wolszczan report DISS observations of PSR 0950+08 at 50 MHz. Their observed δv_d yields predicted RISS m_r of 0.4 and τ_r of 10 days. Our results for this pulsar are thus in agreement for m_r and shorter by a factor of only 3 for τ_r.